Emerging Design Solutions in Structural Health Monitoring Systems

Diego Alexander Tibaduiza Burgos
Universidad Santo Tomás, Colombia

Luis Eduardo Mujica
Universitat Politecnica de Catalunya, Spain

Jose Rodellar
Universitat Politecnica de Catalunya, Spain

A volume in the Advances in Civil and Industrial Engineering (ACIE) Book Series

ENGINEERING SCIENCE REFERENCE
An Imprint of IGI Global

Published in the United States of America by
Engineering Science Reference (an imprint of IGI Global)
701 E. Chocolate Avenue
Hershey PA, USA 17033
Tel: 717-533-8845
Fax: 717-533-8661
E-mail: cust@igi-global.com
Web site: http://www.igi-global.com

Library of Congress Cataloging-in-Publication Data

Emerging design solutions in structural health monitoring systems / Diego Alexander Tibaduiza Burgos, Luis Eduardo Mujica, and Jos? Rodellar, editors.
pages cm
Includes bibliographical references and index.
ISBN 978-1-4666-8490-4 (hardcover) -- ISBN 978-1-4666-8491-1 (ebook) 1. Structural health monitoring. 2. Artificial intelligence--Engineering applications. 3. Structural analysis (Engineering) 4. Structural design. I. Tibaduiza Burgos, Diego Alexander, 1980- editor. II. Mujica, Luis Eduardo, 1976- editor. III. Rodellar, Jos?, editor.
TA656.6.E44 2015
624.1'71--dc23
2015010307

This book is published in the IGI Global book series Advances in Civil and Industrial Engineering (ACIE) (ISSN: 2326-6139; eISSN: 2326-6155)

British Cataloguing in Publication Data
A Cataloguing in Publication record for this book is available from the British Library.

Chapter 11
Prognostics Design for Structural Health Management

J. Chiachío
University of Granada, Spain

S. Sankararaman
SGT Inc., USA & NASA Ames Research Center, USA

M. Chiachío
University of Granada, Spain

A. Saxena
SGT Inc., USA & NASA Ames Research Center, USA

K. Goebel
NASA Ames Research Center, USA

ABSTRACT

The chapter describes the application of prognostic techniques to the domain of structural health and demonstrates the efficacy of the methods using fatigue data from a graphite-epoxy composite coupon. Prognostics denotes the in-situ assessment of the health of a component and the repeated estimation of remaining life, conditional on anticipated future usage. The methods shown here use a physics-based modeling approach whereby the behavior of the damaged components is encapsulated via mathematical equations that describe the characteristics of the components as it experiences increasing degrees of degradation. Mathematical rigorous techniques are used to extrapolate the remaining life to a failure threshold. Additionally, mathematical tools are used to calculate the uncertainty associated with making predictions. The information stemming from the predictions can be used in an operational context for go/no go decisions, quantify risk of ability to complete a (set of) mission or operation, and when to schedule maintenance.

INTRODUCTION

Prognostics is a core element of Prognostics and Health Management (PHM), which sets out to actively monitor and manage assets based on their state of health as opposed to scheduling periodic inspection and maintenance based on statistics of mean-time-to-failure or similar information. Prognostics is the science of determining the remaining useful life (RUL) of a component or subsystem given the current degree of wear or damage, the component's load history, and anticipated load and environmental conditions. A quantification of the degree of a component's wear or damage and the estimate of end-of-life (EOL) gives decision makers important information about the structural health of a system. This information

DOI: 10.4018/978-1-4666-8490-4.ch011

can be used for risk reduction in go/no-go decision, cost reduction through the scheduling of maintenance as-needed, and improved asset availability. Prognostics employs techniques that are often based on an analysis of historical data or an analysis of the fault modes and the modeling of the physics of both the component itself as well as the attributes that characterize the fault. Damage progression models include the effects of damage accelerators or stressors (such as load or environmental conditions). Algorithms that estimate the remaining life use estimation techniques that propagate the anticipated degradation into the future and provide as output the time where the component does no longer meet its desired functionality.

FUNDAMENTALS

Predictive information about a component fault/damage can be a valuable resource in determining an appropriate course of action to avoid failures. Potential of prognostics in positively contributing to safety and improving life-cycle costs is equally relevant to existing legacy systems and new system designs. Legacy systems adopt additional sensing and processing with a potentially high price of retrofitting and additional validation and/or certification costs to gain extended system life and safety factor. New system designs can significantly reduce these costs if prognostics and health management are adopted early in the design to facilitate a more optimal sensor placement for observability and coverage. This, however, requires integration of health management design into the systems engineering process. The following section briefly discusses various design considerations involved in design and development of PHM.

Design Considerations for Prognostics Health Management

With the term "design" one means in general a method of conceiving and planning to realize a solution to a particular engineering problem. This entails formulating a plan and drawing up a scheme how to realize the plan. Generally, the design process is partitioned into the stages

1. Analysis,
2. Concept, and
3. Synthesis.

One needs to start out with having a good understanding of the underlying goals. That is, an understanding of what the prognostic system is meant to accomplish. This could be a reduction of life-cycle cost, or a safety improvement, or an optimization of uptime to better guarantee mission availability or commercial dispatch readiness. The design process is shown in Figure 1 and explained below.

During the *Analysis* phase, requirements for the overall system are created based on the stated goals. Requirements for prognostic system design are guided by the end use of prognostics (Saxena, Celaya, Saha, Saha, Roychoudhury*, et al.*, 2010). There are different motivations for prognostics, such as improving safety, reducing costs, or increasing availability. However, to realize an effective health management system, requirements for prognostics and structural health monitoring (SHM) should be developed with those of the system. This requires forward thinking about what components or subsystems need monitoring and accordingly determine an appropriate sensor network design, which then can be integrated into the structure design in a more cost-effective manner. The application scenario dictates what mitigation action will be most beneficial given a prognostic estimate of remaining-life-of a structure. At the same

Figure 1. Design process of PHM solution
(Goebel, 2014).

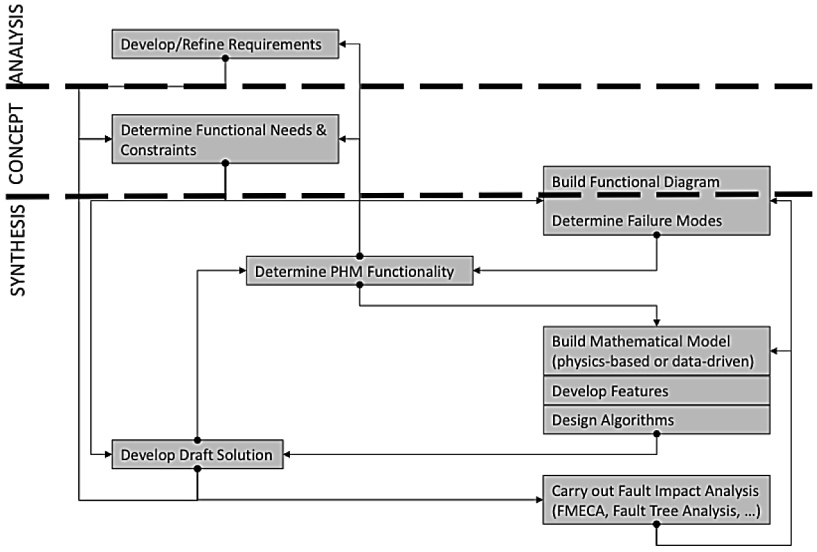

time the benefit achieved by using prognostics also depends on prediction performance. Decisions based on poor predictions can be detrimental in many ways. Late predictions (analogous to false negative) may result in system failures, whereas early predictions (analogous to false positive) trigger unnecessary maintenance actions.

From an engineering design perspective some key factors driving the requirements for prognostics include:

1. Maximum allowable probability of failure of the prognostic system to bound the risk of loss due to failure,
2. Maximum tolerable probability of proactive maintenance to bound unnecessary maintenance,
3. Lead time to specify the amount of advanced warning needed for appropriate actions, and
4. Required confidence to specify when prognosis is sufficiently good to be incorporated into the decision making process.

Keeping these factors in mind the top level system requirements can be translated into prognostic requirements. For instance, the risk posture assumed in a system determines how accurate predictions need to be without increasing the risk of loss beyond acceptable limits. A detailed discussion into deriving prognostics requirements from top level system goals is described in (Saxena *et al.*, 2012). These requirements are generally specified in terms of prediction performance that prognostics must satisfy for desired level of safety or cost benefit.

Next, the functional needs and constraints are evaluated during the *Concept* phase. These will drive a potential solution for which a fault impact analysis will be conducted. This analysis will be used in conjunction with an understanding of the functional operation of the solution approach to define PHM functionality. To that end, functional diagrams representing the desired functions of the subsystem can be used to capture these properties.

During the *Synthesis* phase, the functionality is encapsulated in appropriate models and algorithms that characterize the core of the PHM solution. Checking the degree of fulfillment of requirements may result in changes to the solution before a final choice is made. A clear understanding and representation of the functions that have to be carried out is needed to provide the framework for capturing both how a system operates and how it can fail. It further provides the manifestations of the failure, its consequences, and its impact on the structure as a whole. As the design moves through the synthesis stage and the design takes on shape, the functional diagram is augmented with the failure modes of the physical system. The design is continually analyzed to assess the degree to which it satisfies its requirements. This analysis may evaluate (depending on the goals) observability (i.e., to what degree the detrimental effect can be "seen"); diagnosability (i.e., the ability of the designed PHM system to isolate an anomalous condition to a specific single failure mode or to a group of potential failures called an ambiguity group); coverage (ability of the PHM system to provide indication that the occurrence of a given failure is imminent through the use of prognostics or diagnostics of upstream failures); choice of a method for realizing the observations (e.g., through appropriate sensor placement and information processing); choice of a form of suitable output (status indicators, alarms, reports, etc.); and determination of intended mitigation actions (e.g., report only, decision support, reflexive reconfiguration, repair, etc.). An account of design considerations in the context of integrated vehicle health management is delineated in (SAE, ARP6407).

When PHM methods are applied to structures, which are often subject to a variety of fault modes (cracks, voids, delamination, bondline failures, corrosion, etc.), dedicated sensors and sensor networks are required for observability as no single sensor type can cover all. Composite structures present more challenges due to multiple simultaneous fault modes and their effects in the anisotropic material. Therefore, it can be prohibitively expensive to cover all fault modes in large structures. Well-designed health management solutions carefully identify potential targets for diagnostics and prognostics to optimize costs and benefits. To that end it is a common practice to identify "hot spot" locations and critical fault modes to prioritize targets for prognostics. For instance, from a design perspective it may be decided that all identified hot spots are monitored for fault detection but only some critical ones are considered targets for prognostics. A common analysis tool often employed to identify risks and their consequences is *Failure Modes, Effects, and Criticality Analysis* (FMECA). Using FMECA system designers identify system components that are most likely to cause failures and therefore prioritize monitoring and prognostic targets.

Realizing PHM functions typically includes the need to represent the components of interest with a model, which might be either based on the physical operation of the system or derived from operational data that adequately characterizes the system. This is done after a concept has been chosen. Signal processing methods are employed to derive features from the sensor information that are correlated with the expected response from the model to arrive at an assessment of the health state. Some of the data sources that are utilized include sensor information from sensors that are placed on the components. As mentioned earlier, the sensor information needs to be processed to filter out noise and to derive features that are optimally correlated with the health information of interest. SHM literature covers a wide variety of modeling and sensing solutions for metallic as well as composite structures. A majority of these methods, however, focus on detection techniques and largely stop at damage localization and damage severity estimation. While most sensing and instrumentation commonly used for damage detection and identification in structures is also sufficient for prognostics, there are some unique elements in measurement that must be covered as well. Some of these aspects are discussed below in the context of prognostics.

Sensing for Prognostics

Prognostics is a natural extension of structural health monitoring where the user is not only concerned with detecting, locating, and identifying a fault mode but also determining the remaining time at hand before a failure occurs. It is a continuous process and predictions must be regularly updated as the system health state changes due to further usage. Therefore, operationally prognostics requires frequent measurement updates to continuously estimate structural health and revise predictions of remaining life. Consequently SHM sensors, that can interrogate the system periodically and assess any change in fault severity, are needed for prognostics. While non-destructive inspections can provide valuable trending information, this chapter focuses on largely automated SHM-based prognostics that makes use of permanently installed sensors built into the structure design. Prognostics broadly requires two categories of inputs from monitoring sensors:

1. Damage response measurement;
2. Operational and environmental loading measurement.

The choice of sensing methods or the sensors is primarily guided by what needs to be measured, but is significantly influenced by practical constraints given any application. For example weight, volume and power demand, and cost constraints for sensors onboard airspace systems results in a different sensor choice than for industrial building or bridge structures. Sensor locations are chosen such that the expected type of damage produces known, observable, and statistically significant effects in features derived from the measurements at these locations, which is often determined through numerical simulations or physical tests. Low-level local response caused by damage (e.g., cracks opening and closing) must be separated from large-amplitude global response such as that caused by aerodynamic loads on aircraft by determining required sensitivity and dynamic range through analysis or experimentation.

The following section describes these sensing requirements and common methodologies currently used. Additionally, the need for ground truth measurement for prognostic model development is discussed.

Damage Response Measurement

Prognostic models need information from sensors about degradation or damage in the structures through kinematic (strains, accelerations, etc.) response of the structure. These sensors are also called health monitoring sensors that can detect damage and damage growth, localize damage, assess damage severity, and identify damage types. A variety of sensing technologies has recently surfaced in addition to traditionally used strain and acceleration measurement methods. Among relatively new methods, SHM sensors based on piezoelectric or PZT discs are particularly useful for health monitoring in the context of prognostics. In pitch-catch mode they are used in active interrogation to assess type, location, and degree of damage (Chang *et al.*, 2007; Y. Liu *et al.*, 2010). Integrated into the structure on the surface or embedded into it, PZT sensors allow regular assessment of structural integrity through dynamic strain measurements. A time history of these measurements can inform damage growth model to make predictions of when the structure is expected to reach its failure threshold. Other similar embedded technologies include optical fiber based Fiber Bragg Gratings (FBG), vacuum tube networks, and micro-electro-mechanical systems (MEMS), to name a few.

System Loading Measurement

The other class of sensors characterizes loadings on the system. This includes both operational loading and environmental loading, both of which have an impact on how fast any given damage type grows. These include measurements of static and dynamic loads that the system has experienced and also the environment it has been exposed to. As mentioned in the previous section, this could be achieved by stress monitoring at the key load bearing points identified as prognostic targets. Stresses can be indirectly measured using sensors like strain gauges or be inferred from load calculations using static/dynamic models of the structure and knowledge of the load profile. To characterize environmental loadings such as moisture, temperature, acidity (or pH), etc., the duration of exposure must be monitored. The effect of these factors is then incorporated in the damage growth models used for prognostics.

Damage Ground Truth Measurement

During design and development stages, fault modeling requires access to run-to-failure time series data to understand damage growth characteristics and for model validation. Such data are often difficult to come by as they are rarely collected in practice due to lack of adequate sensing or due to the fact that expensive and critical systems are not allowed to run-to-failure due to safety and cost considerations. Therefore, carefully designed experiments such as accelerated aging are often used to collect such data in representative operational conditions. Another aspect of data collection required for prognostics is measurement of ground truth through non-destructive evaluation (NDE) methods. Commonly used NDE techniques such as X-rays, thermography, ultrasonic A, B, C-Scans etc. are some of the common methods for ground truth measurement.

Performance Evaluations

Within the health management context there are a variety of prediction methods that are generally used to make predictions about system behavior (Saxena *et al.*, 2014). Prognostics is one of those methods that predicts remaining useful life of a specific component or system based on its usage history inferred from monitoring data and expected future load profile. A variety of prognostic performance evaluation metrics have been defined (Saxena, Celaya*, et al.*, 2010b), but as described in (Saxena *et al.*, 2014), prognostic performance must account for three attributes of performance under the presence of uncertainty, namely; Correctness, Timeliness, and Confidence. Correctness deals with accuracy and spread measures of predictions when compared to observed outcomes. Timeliness accounts for how quickly a prediction algorithm produces its outputs, in comparison to the fault growth rate and the time required for enabling a mitigation action. Confidence, on the other hand, is a measure of uncertainty in a prognostic algorithm's output, which is key in making decisions about possible mitigating actions. These attributes are measured through the prediction horizon, the so-called α-λ accuracy (see Equation 1), and relative accuracy measures as described in (Saxena, Celaya*, et al.*, 2010b). These measures not only assess accuracy of predictions but also track performance change with time as predictions are periodically updated.

Prognostics metrics are expressed on a time versus RUL graph, as shown in Figure 2 and Figure 3. Predicted RULs are plotted against time of prediction. The straight line with negative slope represents the true RUL that decreases linearly as time progresses. Ideally predictions should stay on this line as

Figure 2. Illustration of determining Prognostic Horizon metric for two prognostics estimations (Source: Saxena et.al. 2010a).

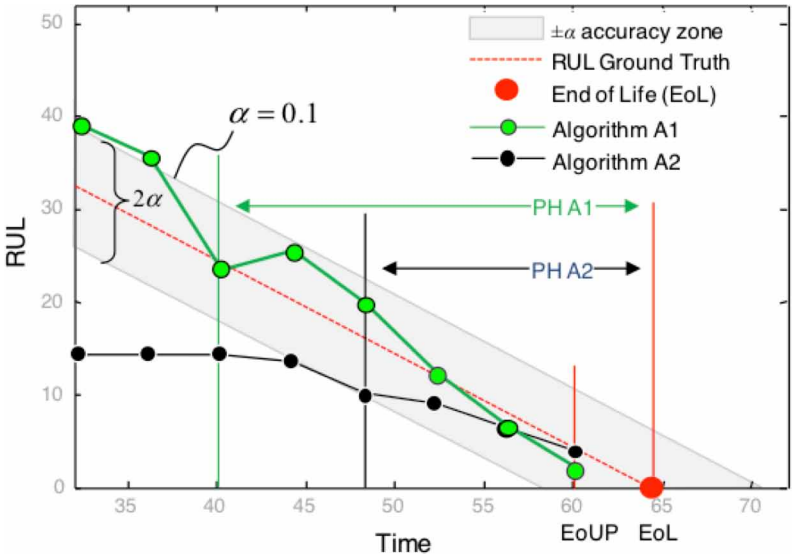

they are updated with time or stay within the accuracy zones specified by parameter α. An advanced version of these metrics considers RUL predictions in the form of PDFs rather than point estimates. These metrics are further parameterized by β, that specifies the minimum acceptable probability of overlap between the predicted RUL and the α accuracy bounds to consider a prediction accurate. Both α and β are design parameters to be determined based on application scenario. Based on these principles, three prognostic measures are briefly described below and further used in the example developed further below.

- **Prognostics Horizon (PH):** Determines the maximum advance warning a prediction algorithm can provide with desired confidence. It is defined as the maximum predicted RUL (or the first prediction) that falls within desired accuracy (α) bounds with an overlap probability larger than parameter β. It can be expressed as the largest RUL value that is accurate to the desired α level. Mathematically, it is defined as $PH = EOL - t_p^*$, such that

$$t_p^* = \min\left\{t \geq 0 : RUL\left(t_p^*\right) \in desired\ accuracy\ \alpha\right\}.$$

- ***α-λ* Performance:** Characterizes how well an algorithm's performance (accuracy and precision) improves as EOL approaches. Improvement is measured against desired accuracy level (α) expressed as a percentage of RUL at any specified time (λ).

$$\alpha - \lambda\ accuracy = \begin{cases} 1 & if\ \ prediction\ \ falls\ inside\ the\ \alpha\ \ accuracy\ cone \\ 0 & otherwise \end{cases} \quad (1)$$

- **Relative Accuracy:** Quantifies how accurate an algorithm is at any given time relative to the EOL. It is computed as RUL error normalized by actual RUL at any given time. It captures the notion that accuracy of prediction becomes more critical as EOL approaches.

Figure 3. Illustration of computation of α-λ accuracy for two prognostics estimations *(Source: Saxena et.al. 2010a).*

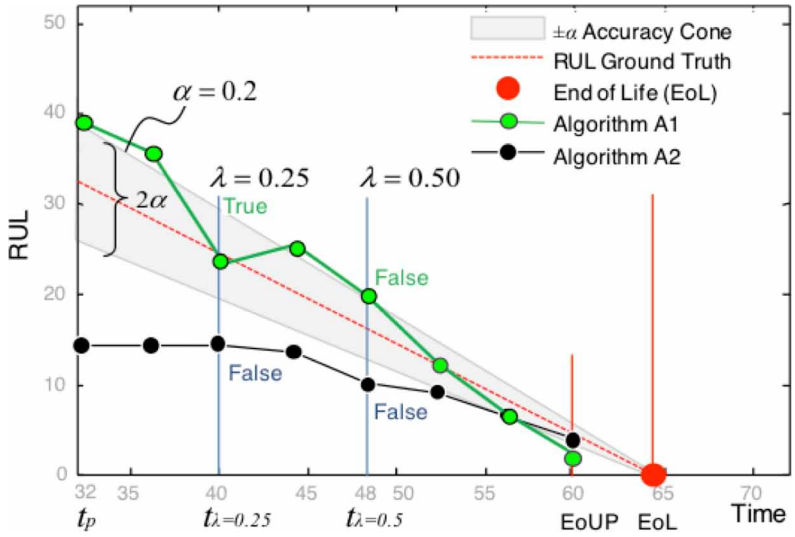

Prognostics Framework

The framework for prognostics hinges on the availability of several elements that are needed for a complete solution. These include a model (typically for both the nominal behavior as well as for the damage behavior), a quantifiable criterion for what constitutes failure, an algorithm to propagate the model to the damage threshold, and a mechanism to deal with uncertainty.

Modeling

As mentioned above, underlying any prediction requires a model that describes how the component of interest behaves under nominal conditions and how it will evolve as it experiences wear or a fault condition. To that end, one needs to represent that process in the form of mathematical equations. This "model" may be derived from laws of physics, encapsulated by empirical relations, or learned from data. Models can also be formed using a combination of these approaches. For example, parts of a component that are well-understood may be constructed using physics-based models, with unknown physical parameters learned from data using appropriate system identification techniques.

Modeling of physics can be accomplished at different levels, for example micro and macro levels. At the micro level, physical models are embodied by a set of dynamic equations that define relationships, at a given time or load cycle, between damage (or degradation) of a component and environmental and operational conditions under which the component is operated. Since measurements of critical damage properties (such as delamination in a composite structure) are rarely available, sensed system parameters have to be used to infer the damage properties. Micro-level models need to account for the assumptions and simplifications in the uncertainty management.

In contrast, macro-level models are characterized by a somewhat abridged representation that makes simplifying assumptions, thus reducing the complexity of the model (typically at the expense of accuracy). An example is a lumped parameter model which assumes that the attributes of the component

have idealized behavior and the non-ideal characteristics are characterized with equivalent elements that suffice for a first-order approximation. When such a system is designed well, it will often (but certainly not always) result in satisfactory results, depending on performance requirements. It should be noted that for complex systems (e.g., a structure with complex geometry and with many different materials), even a macro-level model may be rather time-consuming and labor intensive. The resulting simplifications may need to be accounted for via explicit uncertainty management, which may pose more performance limitations than for a micro-level model.

Nominal System Modeling

The component model describes the characteristics of the component under nominal conditions. Ideally, such a model should be able to factor in the effects of operational and environmental conditions as well as any other conditions that cause different system response under nominal conditions. The model should also be able to adapt to changes of the system that are not considered abnormal. To that end, the system model could learn system behavior from examples, for instance using machine-learning techniques, or it could integrate domain expertise and be implemented using rules.

Damage Propagation Modeling

A damage propagation model describes how the damage is expected to grow in the future. It should, similar to the nominal model, account for operational and environmental conditions as well as any other conditions that have an impact on the damage. Depending on the fault mode, damage propagation may exhibit different symptoms and it may then be necessary to consider dedicated damage propagation models for different fault modes.

Algorithms

The role of the prognostic algorithm is applying the damage propagation model into the future. It needs to ensure that it properly considers the effects of environmental and operational conditions, as well as how to account for the different sources of uncertainty. Depending on the implementation, the damage propagation model and the prognostic algorithm may not be separable. However, for the general case, the damage propagation model and the prognostic algorithm will be treated as separate.

Uncertainty Management

Since prognostics deals with predicting the future behavior of engineering components and systems, it is important to understand that there are several sources of uncertainty that influence future behavior. Therefore, an efficient design for prognostics needs to rigorously account for all these sources of uncertainty to predict the remaining useful life. In the recent past, several researchers have developed different types of methods for uncertainty quantification in prognostics. For example, the Damage Prognosis project (Farrar & Lieven, 2007) at Los Alamos National Laboratory discussed uncertainty in fatigue crack growth by considering different sources of variability, in the context of structural health monitoring. Sankararaman *et al.* (Shankar Sankararaman *et al.*, 2009) developed a computational approach to

account for variability, data uncertainty, and model uncertainty in crack growth prognosis. However, many of these methods are based on offline testing, i.e., testing before and after system operation, and not for condition-based prognostics and monitoring, i.e., prediction during system operation.

Developing methods for uncertainty quantification in the context of condition-based monitoring is challenging because uncertainty methods are generally computationally expensive, whereas condition-based monitoring and prognostics require real time computational power and results for decision-making. An important aspect of condition-based monitoring is the prediction of remaining useful life, and several publications (Engel *et al.*, 2000; Saha & Goebel, 2008) have discussed the importance of quantifying the uncertainty in remaining useful life prediction. Sankararaman *et al*. (S. Sankararaman *et al.*, 2014) discussed sampling methods and analytical methods for estimating the uncertainty in the remaining useful life prediction for prognostics.

Interpreting Uncertainty in Prognostics

Though probabilistic methods have been widely used for uncertainty quantification and management in various engineering applications, the interpretation of probability is, at times, not straightforward. There are two major interpretations of probability: frequentist versus subjective. Frequentist probability assignments are based on the existence of inherent variability and are suitable only in the context of truly random experiments. Traditional statistical principles are primarily based on the concepts of frequentist probability. On the other hand, subjective probabilities express the degree of the analyst's belief regarding a particular statement and can be assigned even in the absence of inherent variability. Principles of Bayesian statistics are based on the concept of subjective probability and are widely used in a variety of engineering applications today.

In the context of health management, the frequentist interpretation of uncertainty is applicable only for testing-based methods. In other words, when several nominally identical specimens are tested, there is inherent variability across them and probabilistic methods are used to quantify this variability. On the other hand, in condition-based prognostics the focus is typically on one particular unit; at any time-instant, this particular unit is in a given state without any associated variability. The uncertainty regarding this state is simply reflective of the degree of belief. Bayesian tracking methods (Kalman filtering, particle filtering, etc.) used for state estimation are called "Bayesian" not only because they use Bayes' theorem for state estimation but also because they are based on subjective probabilities. Similarly, the future loading conditions are also subjective estimates; hence, the resultant remaining useful life also needs to be interpreted subjectively. Thus, it can be clearly seen that the subjective interpretation of uncertainty is consistent across the entire domain of condition-based prognostics (S Sankararaman, 2014).

Sources of Uncertainty

To begin with, it is important to understand the various sources of uncertainty that affect calculations in prognostics. It has been conventional to classify the different sources of uncertainty into aleatory (physical variability) and epistemic (lack of knowledge), where epistemic uncertainty consists of data uncertainty and model uncertainty. However, in the case of condition-based monitoring, there is only one particular system being monitored, and not multiple realizations of a population, and therefore, it is not meaningful to discuss variability. For example, the system is at a particular state at any time in-

stant and there is nothing variable about it. Variability would need to be accounted for only in the case of reliability-testing methods where multiple components/systems are tested. Therefore, the sources of uncertainty in prognostics are classified into:

- **Modeling Uncertainty:** Predicting the future is the most important aspect of prognostics, and typically, a physics-based model or a data-driven model is used for predicting future behavior. This model is usually represented using state-space equations. Modeling uncertainty represents the difference between the predicted response and the true response (which can neither be known nor measured accurately), and comprises of several parts such as model parameters, model class, process noise, etc.
- **Present Uncertainty:** The first step of prognostics is to estimate the condition/state of the component/system at any time instant. Output data (collected through sensors) is used to estimate the current state and many filtering approaches are able to estimate the state, and calculate the uncertainty associated with the state estimate.
- **Future Uncertainty:** The most important source of uncertainty in the context of prognostics is due to the fact that the future is unknown, i.e. both the loading and operating conditions are not known precisely. The future behavior (i.e., the response of the system to the loading and operating conditions) needs to be estimated using a model; the usage of a model imparts additional uncertainty as explained earlier.

Uncertainty-Related Activities in PHM

Having explained the various sources of uncertainty, it is important to define a series of activities that can be collectively used to address these sources of uncertainty in a systematic manner. In the context of prognostics and health management, uncertainty has been discussed from the perspectives of quantification, representation, and management, in various publications (Orchard *et al.*, 2008; Tang *et al.*, 2009). While all the three are different processes, they are often confused with each other and interchangeably used (Celaya *et al.*, 2012). For the purpose of clarity, four different uncertainty-related activities are detailed below:

1. **Uncertainty Representation and Interpretation:** The first step is the representation of uncertainty, which may be guided by the choice of the modeling and simulation framework. There are several methods for uncertainty representation that vary in the level of granularity and detail. A probabilistic framework is used for uncertainty representation in this chapter, and the interpretation of this uncertainty is discussed shortly.
2. **Uncertainty Quantification:** The second step of uncertainty quantification deals with identifying and characterizing the various sources of uncertainty that can prospectively affect the prognostic calculations.
3. **Uncertainty Propagation:** The third step of uncertainty propagation is most relevant to prognostics, since it accounts for all the uncertainties previously quantified and uses this information in order to predict the future behavior, remaining useful life, and the associated uncertainty.
4. **Uncertainty Management:** The fourth and final step is uncertainty management, and it is unfortunate that, in several articles, the term "Uncertainty Management" has been used instead of uncertainty quantification and/or propagation. As a result, there are few publications that directly

address the issue of uncertainty management. In general, uncertainty management is a term used to refer to different activities that aid in managing uncertainty in condition-based maintenance during real-time operation. There are several aspects of uncertainty management. One aspect of uncertainty management attempts to answer the question: "Is it possible to improve the uncertainty estimates?" The answer to this question lies in identifying which sources of uncertainty are significant contributors to the uncertainty in the RUL prediction. Another aspect of uncertainty management deals with how uncertainty-related information can be used in the decision-making process.

A PROGNOSTICS DESIGN SOLUTION

A general computational framework for prognostics and health management is presented in this section. Let us consider an engineering component or system such that, at any generic time-instant t_p, it is desired to perform prognostics and predict the remaining useful life. Figure 4 provides a conceptual scheme of the proposed prognostics framework, which consists of the following three sub-problems:

1. Present state estimation;
2. Future state prediction;
3. RUL computation.

In order to address the above problems, a generic time-dependent, state-space modeling framework is firstly presented. This framework needs to account for the different sources of uncertainty as explained in the previous section, and therefore, the state-space models also need to account for the various sources of uncertainty.

Stochastic System Modeling for Prognostics

Consider a general engineering component/system whose damage response can be modeled as

$$\frac{dx(t)}{dt} = g\left(t, x(t), u(t), \theta\right) + v(t) \tag{2}$$

where $x(t) \in \mathbb{R}^{n_x}$ is the state vector (that depicts the state of the system at any time instant), $\theta \in \mathbb{R}^{n_\theta}$ is the parameter vector (parameters of the model), $u(t) \in \mathbb{R}^{n_u}$ is the input vector (loadings, environmental conditions, operating conditions, etc.), $v(t) \in \mathbb{R}^{n_x}$ is the model error vector (used to represent unmod-

Figure 4. Prognostics architecture; a description of the mathematical symbols is provided further below.

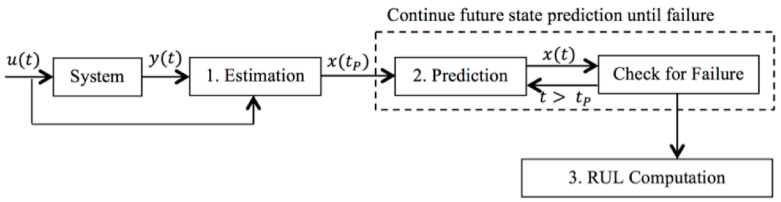

eled random variations in the engineering component/system), and $g \in \mathbb{R}^{n_x}$ is the state transition equation.

The above differential equation simply predicts how the state of a system continuously progresses as a function of time, loading conditions, model parameters, etc. Typically, in the context of prognostics and health management, a state variable or a collection of state variables are used to represent the health state of the system. Usually, the health of a system deteriorates as a function of time, and therefore, it can be estimated by quantifying the states of the system; hence, tracking the states is essential to tracking the health of the system.

As discussed in the last section, there are several sources of uncertainty that affect the performance of the system, and all of these sources of uncertainty can be included in this modeling framework. For example, certain characteristics of the system are represented using parameters and it may not be able to know these quantities precisely; therefore the parameters ($\boldsymbol{\theta}$) are uncertain. In addition, external input factors (u) such as loading conditions, operating conditions, etc. may not be known precisely or cannot be controlled. In fact, all of the variables in the above state-space modeling framework are uncertain and need to be modeled using probability distributions. As mentioned earlier, in many cases, such uncertainty must not be confounded with variability, particularly in the context of condition-based prognostics. Due to these different sources of uncertainty, the state estimates available through the estimation procedure will also become uncertain. It is important that the state estimation procedure rigorously accounts for these sources of uncertainty and accurately computes their effect on the state estimate. As a result, the state estimation procedure represents the system state using probability distributions.

State estimation is accomplished by continuously collecting measurements of the output variables through sensors, where these measurements are available until the time of prediction denoted by t_P. Then, along with the above state prediction model, an output-measurement model can also be defined as:

$$y(t) = h\left(t, x(t), u(t), \theta\right) + w(t) \tag{3}$$

where $y(t) \in \mathbb{R}^{n_y}$ is the output vector (measurements available through sensors until $t = t_P$), $w(t) \in \mathbb{R}^{n_y}$ is the measurement noise vector, and $h \in \mathbb{R}^{n_y}$ is the output equation.

Using recursively Equations (2) and (3), the state estimate at time of prediction $x(t_P)$ can be calculated using an accurate state estimation procedure, as shown further below.

Bayesian State Estimation

As stated before, many problems in a variety of areas of science and engineering can be expressed using a state space model, as defined by Equations (2) and (3). In general, for the purpose of prognostics, this state-space model is usually converted into a discrete-time system by using numerical integration over a sufficiently small time step Δt, leading to a hidden Markov model, as follows:

$$x_n = g_n\left(x_{n-1}, u_n, \theta\right) + v_n \tag{4}$$

$$y_n = h_n\left(x_n, u_n, \theta\right) + w_n \tag{5}$$

where $x_n = x(n \cdot \Delta t)$ and $y_n = y(n \cdot \Delta t)$ are the latent (or hidden) state and the measured response of the system at time $n \cdot \Delta t$; and $u_n = u(n \cdot \Delta t)$, $v_n = v(n \cdot \Delta t)$ and $w_n = w(n \cdot \Delta t)$ are the input vector, model error and measurement error at time $t = n \cdot \Delta t$, respectively. The sequence of states $\left\{x_n; n \in \mathbb{N}\right\}$ is assumed to follow a hidden Markov process, while the observations $\left\{y_n; n \in \mathbb{N}\right\}$ are conditionally independent given the process $\left\{x_n; n \in \mathbb{N}\right\}$. From now on, time will be denoted by the index n since it is sufficient to indicate which time is being considered.

The goal of Bayesian state estimation is to sequentially estimate the PDF of the sequence of latent states $x_{0:n} \triangleq \left\{x_0, \ldots, x_{n-1}, x_n\right\}$ given a sequence of measurements up to time n, denoted by $y_{0:n} \triangleq \left\{y_0, \ldots, y_{n-1}, y_n\right\}$. This PDF is typically known as the *posterior*, expressed as $p\left(x_{0:n} \mid y_{0:n}, \theta\right)$, since it is obtained from the last available state estimation, known as the prior PDF, $p\left(x_{0:n-1} \mid y_{0:n-1}, \theta\right)$. Hereinafter, and without loss of generality, input parameters u_n will be dropped from the formulation for the sake of simpler notation.

In the state space modeling literature, the posterior PDF is commonly studied through one of its marginals, the so-called filtering distribution, $p\left(x_n \mid y_{0:n}, \theta\right)$. To obtain this distribution, a two-stage recursive approach is typically formulated:

1. The prediction stage, in which the one-step ahead predictive PDF $p\left(x_n \mid y_{0:n-1}\right)$ is estimated based on available data up to time $n-1$ using Total Probability Theorem, and
2. The updating stage, in which the former PDF is updated to get the posterior PDF $p\left(x_n \mid y_{0:n}\right)$ based on a new measurement at time n, using Bayes' Theorem. That is:

$$\begin{aligned} p\left(x_n \mid y_{0:n-1}, \theta\right) &= \int p\left(x_n \mid x_{n-1}, \theta\right) p\left(x_{n-1} \mid y_{0:n-1}, \theta\right) dx_{n-1} \\ p\left(x_n \mid y_{0:n}, \theta\right) &= \frac{p\left(y_n \mid x_n, \theta\right) p\left(x_n \mid y_{0:n-1}, \theta\right)}{\int p\left(y_n \mid x_n, \theta\right) p\left(x_n \mid y_{0:n-1}, \theta\right) dx_n} \end{aligned} \tag{6}$$

Continually iterating between the equations in (6) constitutes the basis of sequential state estimation. However, this recursive scheme is only a theoretical solution given that, in general, the integrals involved in these equations cannot be calculated analytically, except for some especial cases. The first special case is when Equations (4) and (5) involve linear functions and errors v_n and w_n are Gaussians. In this case, an analytical solution can be obtained for the recursions in (6) using the well-known Kalman filter (Kalman, 1960). The other case is when the state variable x_n can be represented by a discrete set of values, where grid-based methods (Arulampalam *et al.*, 2002) can be applied to efficiently solve the system in (6). For the general case, Sequential Monte Carlo (SMC) methods (Doucet *et al.*, 2001) can be used to efficiently solve these iterations avoiding the calculation of the aforementioned multidimensional integrals, as shown further below.

When the interest is instead in obtaining the posterior PDF $p\left(x_{0:n} \mid y_{0:n}\right)$, then Bayes' Theorem can be applied to update the last posterior a time $n-1$, as follows:

$$\begin{aligned} p\left(x_{0:n} \mid y_{0:n}, \theta\right) = & \quad p\left(x_{0:n} \mid y_n, y_{0:n-1}, \theta\right) \\ \propto & \quad p\left(y_n \mid x_{0:n}, y_{0:n-1}, \theta\right) p\left(x_{0:n} \mid y_{0:n-1}, \theta\right) \\ \propto & \quad p\left(y_n \mid x_n, \theta\right) p\left(x_n \mid x_{n-1}, \theta\right) \underbrace{p\left(x_{0:n-1} \mid y_{0:n-1}, \theta\right)}_{last\ \ updating} \end{aligned} \tag{7}$$

In equations (6) and (7) it is assumed that $p\left(x_n \mid x_{0:n-1}\theta\right) = p\left(x_n \mid x_{n-1}, \theta\right)$ since Equation (4) describes a Markov model of order one, i.e., the process is conditionally dependent on the past sequence only through the last state. In addition, it is assumed that the probability models for error terms v_n and w_n are given, and as a consequence, the PDFs for the state transition equation and observation equation are prescribed. For example, when v_n and w_n are modeled as zero-mean Gaussian distributions, which is supported by the Principle of Maximum Information Entropy (PMIE) (Jaynes, 1983), then the transition equation and the observation equation in (4) and (5) can be expressed as Gaussian distributions, as:

$$p\left(x_n \mid x_{n-1}, \theta\right) = \left((2\pi)^{n_x} \mid \Sigma_{v_n} \mid\right)^{-\frac{1}{2}} \exp\left(-\frac{1}{2}\left(x_n - \overline{x}_n\right)^T \Sigma_{v_n}^{-1}\left(x_n - \overline{x}_n\right)\right) \tag{8}$$

$$p\left(y_n \mid x_n, \theta\right) = \left((2\pi)^{n_y} \mid \Sigma_{w_n} \mid\right)^{-\frac{1}{2}} \exp\left(-\frac{1}{2}\left(y_n - \overline{y}_n\right)^T \Sigma_{w_n}^{-1}\left(y_n - \overline{y}_n\right)\right) \tag{9}$$

where $\overline{x}_n = g_n\left(x_{n-1}, u_n, \theta\right)$ and $\overline{y}_n = h_n\left(x_n, u_n, \theta\right)$, being $\Sigma_{v_n} \in \mathbb{R}^{n_x \times n_x}$ and $\Sigma_{w_n} \in \mathbb{R}^{n_y \times n_y}$ the covariance matrices of the model error and the measurement error, respectively. As shown in Equations (6) and (7), the two last probability models $p\left(x_n \mid x_{n-1}, \theta\right)$ and $p\left(y_n \mid x_n, \theta\right)$ are fundamental elements in the Bayesian state estimation problem explained in this section.

Joint State-Parameter Estimation

To better estimate the current damage state of the system, and more importantly, to reduce the uncertainty of the future predictions about the system, a followed solution is to sequentially update both states and model parameters using the sequential state estimation framework presented above. In doing so, the system equations g_n and h_n are expected to provide more accurate predictions as long as model parameters are allowed to learn from data. To deal with the Bayesian state estimation problem for both states and parameters, an augmented state $z_n = \left(x_n, \theta_n\right) \in \mathbb{R}^{n_x + n_\theta}$ is usually defined so that the same fundamental equations defined in (7) can be redefined to obtain the posterior PDF for the augmented state, i.e., $p\left(z_{0:n} \mid y_{0:n}\right)$, as follows:

$$\begin{aligned} p\left(z_{0:n} \mid y_{0:n}\right) = & \quad p\left(z_{0:n} \mid y_n, y_{0:n-1}\right) \\ \propto & \quad p\left(y_n \mid z_{0:n}, y_{0:n-1}\right) p\left(z_{0:n} \mid y_{0:n-1}\right) \\ \propto & \quad p\left(y_n \mid z_n\right) p\left(z_n \mid z_{n-1}\right) p\left(z_{0:n-1} \mid y_{0:n-1}\right) \end{aligned} \tag{10}$$

where

$$p\left(z_n \mid z_{n-1}\right) = p\left(x_n \mid x_{n-1}, \theta_n\right) p\left(\theta_n \mid \theta_{n-1}\right) \tag{11}$$

$$p\left(y_n \mid z_n\right) = p\left(y_n \mid x_n, \theta_n\right) \tag{12}$$

A key problem that typically arises when sequentially updating the joint state-parameter vector $z_{0:n} = \left\{x_{0:n}, \theta_{0:n}\right\}$ as an augmented state is the non-dynamics nature of θ, which makes it difficult to obtain the required PDF $p(\theta_n \mid \theta_{n-1})$ and therefore, to explore the space of parameters. A common solution consists in adding an independent random perturbation ξ_n to the set of updated parameters at time $n-1$, before evolving to the next state at time n, i.e., $\theta_n = \theta_{n-1} + \xi_n$. This induces a Markovian-type artificial dynamics (Gordon *et al.*, 1993; J. Liu & West, 2001) to model parameters, from which the PDF $p\left(\theta_n \mid \theta_{n-1}\right)$ is prescribed. For example, in the common case of ξ_n being modeled as a white noise (zero-mean Gaussian), the PDF for artificial evolution of model parameters can be obtained as:

$$p\left(\theta_n \mid \theta_{n-1}\right) = \mathcal{N}\left(\theta_{n-1}, \Sigma_{\xi_n}\right) \tag{13}$$

where $\Sigma_{\xi_n} \in \mathbb{R}^{n_\theta \times n_\theta}$ is the covariance matrix of the *random walk* defined in the last equation. Observe that by using this method the model parameters are virtually time evolving although they are essentially not dependent on time. This time varying imposes a loss of information in θ over time (i.e. larger spread) since additional uncertainties are artificially added to model parameters, which ultimately influences the precision of the state estimation. There exist several methods in the literature to overcome this drawback, being the most popular those that impose some kind of shrinkage over Σ_{ξ_n} as long as new data is collected (J. Liu & West, 2001). An efficient method in this direction has been recently proposed by Daigle and Goebel (M. J. Daigle & Goebel, 2013) consisting in modifying the variance of the random walk by adding a negative scalar proportional to the relative difference between the actual and the target spread of the marginal posterior $p\left(\theta_{n,j} \mid y_{0:n}\right)$, with $\theta_{n,j}$ the j^{th} component of the parameter vector θ_n, as follows:

$$\sigma^2_{\xi_{n,j}} = \sigma^2_{\xi_{n-1,j}} \left(1 - P^*_j \frac{RMAD\left(\theta_{n,j}\right) - RMAD^*_j}{RMAD\left(\theta_{n,j}\right)}\right) \tag{14}$$

where $\mathrm{RMAD}\left(\theta_{n,j}\right)$ is the *Relative Median Absolute Deviation* of $p\left(\theta_{n,j} \mid y_{0:n}\right)$, $RMAD_j^*$ is the required or target RMAD for $p\left(\theta_{n,j} \mid y_{0:n}\right)$, and $P_j^* \in \left[0,1\right]$ is a constant that tunes the speed of convergence to $RMAD_j^*$. The reader is referred to (M. J. Daigle & Goebel, 2013) for details about the optimal choice for P_j^* and $RMAD_j^*$. The term $\mathrm{RMAD}(\theta_{n,j})$ can be readily calculated using samples from the marginal posterior $\tilde{\theta}_{n,j} = \left\{\theta_{n,j}^{(1)},\ldots,\theta_{n,j}^{(k)},\ldots,\theta_{n,j}^{(K)}\right\} \sim p\left(\theta_{n,j} \mid y_{0:n}\right)$, as follows:

$$RMAD\left(\theta_{n,j}\right) = \frac{median\left(\left\{\left|\theta_{n,j}^{(k)} - median\left(\tilde{\theta}_{n,j}\right)\right|\right\}_{k=1}^{K}\right)}{median\left(\tilde{\theta}_{n,j}\right)} \tag{15}$$

The proposed method for joint state-parameter estimation is presented as Algorithm 1 at the end of this section.

Future State Prediction

Having calculated the probability distribution of the state estimate at the time of prediction *n*, the next step for prognostics is to predict the distribution of future states of the system ℓ steps forward in time (measured using time-indices) in absence of new measurements.

In this context, the resultant distribution is known as the $\ell-$step-ahead predictive PDF, defined mathematically as $p\left(z_{n+\ell} \mid y_{0:n}\right)$ where $\ell \in \mathbb{N} > 1$. Using the up-to-date information of the system based on the filtering distribution $p\left(z_n \mid y_{0:n}\right)$ and the dynamics of the system, which is encapsulated in the state transition equation defined in Equation (11), the $\ell-$steps-ahead prediction of the system health state $p\left(z_{n+\ell} \mid y_{0:n}\right)$ can be formulated using Total Probability Theorem as follows:

$$\begin{aligned} p\left(z_{n+\ell} \mid y_{0:n}\right) &= \int_{\mathcal{Z}} p\left(z_{n+\ell} \mid z_{n:n+\ell-1}\right) p\left(z_{n:n+\ell-1} \mid y_{0:n}\right) dz_{n:n+\ell-1} \\ &= \int_{\mathcal{Z}} \prod_{l=n+1}^{n+\ell} p\left(z_l \mid z_{l-1}\right) p\left(z_n \mid y_{0:n}\right) dz_{n:n+\ell-1} \end{aligned} \tag{16}$$

It should be noted that the last multidimensional integral is analytically intractable, however it can be readily approximated by the use of sampling-based methods, as shown further below in this section.

Defining EOL and RUL

At this juncture, once the problem of future state prediction has been assessed, the next natural step for prognostics is to estimate the EOL and RUL of the engineering component/system. To this end, a mathematical description of the aforementioned terms EOL and RUL is previously introduced. For the sake of generality, these concepts are explained here using continuous time notation instead of the discrete-index notation, useful from the implementation perspective. However, recall that there exist a one-to-one

mapping between continuous time t and discrete time-index n (e.g., $t = n \cdot \Delta t$, being Δt a sufficiently small time-step) and thus the EOL and RUL could also be expressed in terms of discrete time.

Let define the region $\mathcal{A}$ of acceptable performance as a subspace of the joint state-parameter-inputs space $\mathcal{Z} \subset \mathbb{R}^{n_x} \times \mathbb{R}^{n_\theta} \times \mathbb{R}^{n_u}$. This region can be defined by means of a set of n_c constrains or thresholds, $C_{EOL} = \left\{c_i\right\}_{i=1}^{n_c}$, where each threshold $c_i \in C_{EOL}$ is a function that maps a given point $\left(x(t), \theta(t), u(t)\right) \in \mathcal{Z}$ into the Boolean domain $\mathcal{B} \triangleq \{0,1\}$, i.e. $c_i : \mathcal{Z} \rightarrow \mathcal{B}$, being $c_i\left(x(t), \theta(t), u(t)\right) = 1$ when the constrain is satisfied and 0 otherwise (Shankar Sankararaman *et al.*, 2013). These individual constrains may be combined into a single threshold function $T_{EOL} : \mathcal{Z} \rightarrow \mathcal{B}$ that can be mathematically defined as:

$$T_{EOL}\left(x(t), \theta(t), u(t)\right) = \begin{cases} 1 & if\ 0 \in \left\{c_i\left(x(t), \theta(t), u(t)\right)\right\}_{i=1}^{n_c} \\ 0 & otherwise \end{cases} \tag{17}$$

In other words, $T_{EOL} = 1$ when any of the constraints is violated, and 0 otherwise. Therefore, the End-of-Life at the time of prediction t_p, denoted by $EOL\left(t_p\right)$, can be calculated as the earliest time $t \geq t_p$ for which $T_{EOL} = 1$. In mathematical terms:

$$EOL\left(t_p\right) = \inf\left\{t \in \mathbb{R}^+ : t \geq t_p \wedge T_{EOL}\left(x(t), \theta(t), u(t)\right) = 1\right\} \tag{18}$$

In Figure 5, a schematic illustration of the trajectory of a general state $x(t)$ is provided along with the region $\mathcal{A}$ of acceptable performance (in gray color). Note that the state is propagated forward in time from the time of prediction t_p until the boundary of the acceptable performance region is reached. The first "hitting" time t at which that happens defines the EOL. Having computed the EOL, the remaining useful life at the time of prediction can be readily calculated as:

$$RUL\left(t_p\right) = EOL\left(t_p\right) - t_p \tag{19}$$

Note from Equation (19) and preceding equations that an estimation of RUL at an arbitrary time of prediction depends on the following quantities:

- State estimate at time of prediction, $x(t_p)$.
- Future loading conditions $u(t)$, where $t \geq t_p$. Both environmental and operating conditions may be described along with loading conditions by the vector $u(t)$.
- Future values for model parameters, $\theta(t)$.
- Future values for model error, $v(t)$.

For the purpose of RUL prediction, all of the above quantities are functionally independent of each other; hence, RUL becomes a functionally dependent quantity, as shown in Figure 6. Let $X = \left(X_1, X_2, ..., X_m\right)$

Figure 5. Conceptual two-dimensional example of system trajectory to EOL

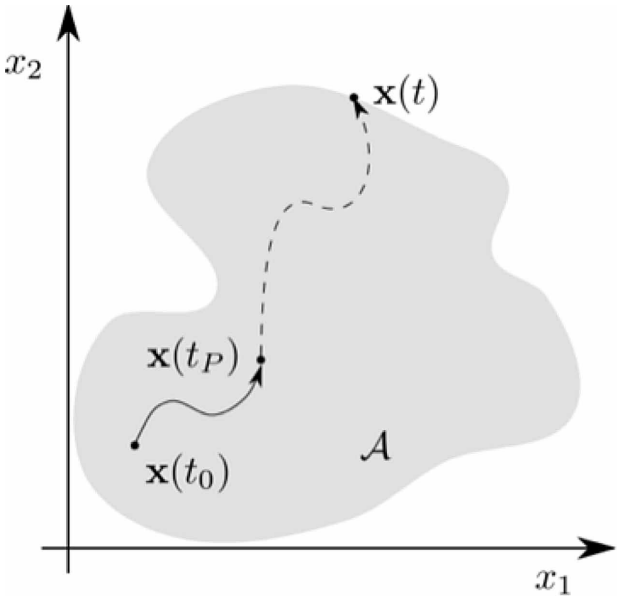

denote the vector of all of the above quantities, where *m* is the length of the vector X, i.e., the number of quantities influencing the RUL prediction. Then, the RUL can be expressed analytically by:

$$RUL = f(X) \tag{20}$$

In view of Equation (20), for every realization of *X* it is possible to compute the corresponding realization of *RUL*. However, as explained earlier, all of these quantities are uncertain and therefore, *RUL* is unavoidably uncertain. In order to account for the uncertainty in the remaining useful life estimation, it is necessary to propagate the uncertainty in *X* through *f*. It has been recently demonstrated that such uncertainty propagation is non-trivial even when the state-space models are linear and the uncertain variables follow Gaussian distributions. This is because the combination of the state-space model and the threshold function will always render *f* as a non-linear function (S. Sankararaman *et al.*, 2014). Hence, it is necessary to resort to statistical approaches in order to estimate the probability distribution of RUL. These methods can be roughly classified into three types: sampling-based methods, analytical methods, and hybrid methods. While some of them may calculate the cumulative distribution function (CDF) of RUL, denoted by $F_{RUL}(t) = P(RUL \le t)$, other methods directly generate samples from it and use these samples to construct an estimation of the probability density function of RUL, denoted by $p(RUL)$. These methods are summarized below.

Sampling-Based Methods

The most intuitive method for uncertainty propagation is to make use of Monte Carlo simulation (MCS). The fundamental concept of MCS (Caflisch, 1998) is to generate pseudo-random number that is uniformly distributed on the interval [0, 1]; therefore the CDF of *X* is inverted to generate several random

Figure 6. Scheme for RUL computation

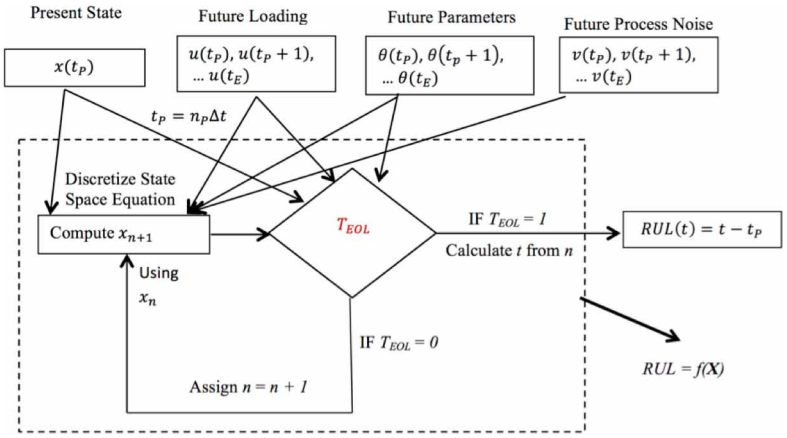

realizations of *X* whereby the corresponding random realizations of *RUL* are computed. Then the CDF $F_{RUL}(t)$ is calculated as the proportion of realizations such that $RUL \leq t$. The generation of each realization requires one evaluation/simulation of Equation (20). Several thousands of realizations may often be needed to calculate the entire CDF, especially for very high/low values of t. Error estimates for the CDF in terms of the number of simulations are well-known in the literature, see for example (Haldar & Mahadevan, 2000). Alternatively, the PDF *p(RUL)* can be computed based on the available samples from Equation (20) using kernel density estimation (Rosenblatt & others, 1956).

More sophisticated methods such as particle filtering (PF) (Gordon *et al.*, 1993) can be used to simply propagate the resultant "particles" into the future. Such approach is only slightly different from MCS where the difference resides in that the particles have their own weights. In order to accurately capture the entire probability distribution of RUL, it may be necessary to employ large amounts of "particles" which necessarily increases the computational cost. Henceforth, such an approach may not be suitable for online health monitoring and prognostics in complex systems. This is why it is necessary to further investigate new efficient sampling-based methods that can significantly improve the computational effort. Some of these sampling-based methods are:

- **Importance Sampling:** This algorithm (Glynn & Iglehart, 1989) does not generate random realizations of *X* from the original distribution. Instead, random realizations are generated from a proposal density function. Statistics of *RUL* are estimated and then corrected based on the values from the original density and the proposal density.
- **Adaptive Sampling:** This method (Bucher, 1988) is an advanced sampling technique where the efficiency of importance sampling is continuously improved by updating the proposal density function based on the information obtained after evaluating *f* for a few samples. Two classes of adaptive sampling methods are multi-modal sampling (Karamchandani *et al.*, 1989) and curvature-based sampling (Wu, 1994). It has been demonstrated (Haldar & Mahadevan, 2000) that adaptive sampling techniques can accurately estimate the failure probability using hundreds of samples whereas traditional Monte Carlo techniques typically require several hundreds of thousands of samples.

- **Stratified Sampling:** In this sampling approach, the overall domain of *X* is split into multiple sub-domains and samples are independently drawn from each sub-domain. The process of dividing the overall domain into multiple sub-domains is referred to as stratification. This method is applicable when subpopulations within the overall population are significantly different.
- **Latin Hypercube Sampling:** This is a sampling method commonly used in design of computer experiments (Loh, 1996). When sampling a function of m_1 variables, the range of each variable is divided into m_2 equally probable intervals, thereby forming a rectangular grid. Then, sample positions are chosen such that there is exactly one sample in each row and column of this grid. Each resultant sample is then used to compute a corresponding realization of *RUL*, and thereby the PDF *p(RUL)* can be calculated.
- **Unscented Transform Sampling:** Unscented transform sampling (M. Daigle *et al.*, 2012; Van Zandt, 2001) is a sampling approach that focuses on estimating the mean and variance of *RUL*, instead of the entire probability distribution. Certain pre-determined sigma points are selected in the *X*-space and these sigma points are used to generate corresponding realizations of *RUL*. Using weighted averaging principles, the mean and variance of *RUL* are calculated.
- **Subset Simulation:** Subset Simulation is an adaptive stochastic simulation approach originally conceived to compute small failure probabilities of engineering systems (Au & Beck, 2001). The conceptual idea behind Subset Simulation is to represents a small failure probability as a product of larger probabilities. Recently, (M. Chiachio *et al.*, 2014) have proposed a new algorithm called "PFP-SubSim" that exploits the benefits of Subset Simulation into the prognostics procedure, and has demonstrated high efficiency for the prognostics of rare-events.

Analytical Methods

A class of analytical methods was developed in the field of structural engineering to perform uncertainty propagation without the need to employ repetitive evaluations. These methods facilitate a quick (in terms of number of evaluations of function *f*) and efficient (reasonably accurate) calculation of the probability distribution of *RUL*.

- **First Order Second Moment Method:** This method (Dolinski, 1983) uses only the mean and variance of all the uncertain quantities and the first-order Taylor's series expansion of *f*, in order to calculate the mean and variance of the response quantity *RUL*.
- **First Order Reliability Method:** This method calculates the CDF function $F_{RUL}\left(t\right)$ by linearizing *f* around the so-called most probable point (Haldar & Mahadevan, 2000; M Hohenbichler & Rackwitz, 1983; Shankar Sankararaman *et al.*, 2013). By repeating this calculation for multiple values of *t*, the entire CDF can be obtained. While this approach is an approximation, it has been demonstrated that it can estimate the CDF with reasonable accuracy in many practical applications (Haldar & Mahadevan, 2000; Shankar Sankararaman *et al.*, 2013).
- **Inverse First Order Reliability Method:** This method is the inverse of the first-order reliability method, i.e., it calculates the value of *t* that corresponds to a given value of β such that $F_{RUL}\left(t\right) = \beta$. By repeating this approach for several values of β, the entire cumulative distribution function of *RUL* can be easily calculated, thereby estimating the uncertainty in *RUL*.

- **Second Order Reliability Method:** The second order reliability method (Der Kiureghian *et al.*, 1987) improves the estimate of the first-order reliability method through a quadratic approximation of *f*, instead of using a linear approximation. There are different types of quadratic approximations and corresponding second-order reliability estimates, thereby leading to a variety of computational methods as those proposed by Kiureghian et al. (Der Kiureghian *et al.*, 1987), Tvedt (Tvedt, 1989), Hohenbichler and Rackwitz (Michael Hohenbichler & Rackwitz, 1988), etc.

Hybrid Methods

In addition to the sampling-based methods and analytical methods, there are also a class of methods called hybrid methods that combine both sampling and the use of analytical tools. Typically these methods are of the form of surrogate models where few samples of *X* and the corresponding values of *RUL* are computed and further used by basis functions (or interpolating functions) in order to facilitate the evaluation of *f* at untrained locations of *X*. Such surrogate modeling approaches include regression techniques (Haldar & Mahadevan, 2000) polynomial chaos expansion (Najm, 2009), kriging (Dwight & Han, 2009), among others.

Summary

In summary, while the aforementioned uncertainty propagation methods have been used in different types of engineering applications, it is still necessary to investigate their applicability to prognostics. Further, note that uncertainty propagation is still a challenging problem in several practical applications due to the limitations of the aforementioned methods. It is rarely possible to accurately calculate the actual probability distribution of RUL by analytical methods. Accurate calculation is possible when using infinite samples by Monte Carlo sampling. Any other method (even the use of a limited, finite number of samples) will lead to uncertainty in the estimated probability distribution, and this additional uncertainty is referred to as prediction-method uncertainty. It is possible to decrease (and maybe, eventually eliminate) this type of uncertainty either by using advanced probability techniques or powerful computing power.

Algorithms for Prognostics

Having discussed a variety of methods for prognostics, this section presents two algorithms for sequential state estimation and RUL prediction, respectively. Both of them are widely used by the prognostics community for their versatility and ease of implementation.

As explained before, the Bayesian state estimation methodology presented earlier in this section is analytically intractable except some especial cases mentioned above (Arulampalam *et al.*, 2002). An alternative for the general case of both non-linear and non-Gaussian state-space models, and non-discretizable state variable, is by the use of Sequential Monte Carlo (SMC) methods (Arulampalam *et al.*, 2002; Cappé *et al.*, 2007; Doucet *et al.*, 2001; Gordon *et al.*, 1993) for drawing samples from the posterior PDF $p\left(z_{0:n} \mid y_{0:n}\right)$ avoiding the calculation of the multidimensional integrals in Equations (6) and (7). A comprehensive treatment of SMC methods can be found in (Doucet *et al.*, 2001). As a special case of SMC methods, particle filters (PF) (Gordon *et al.*, 1993) emerge as the state-of-art of SMC algorithms for sequential state estimation. These methods share a common principle of approximating the

required posterior PDF through a set of N discrete samples or *particles* $\left\{z_{0:n}^{(i)}\right\}_{i=1}^{N}$ with associated set of *weights* $\left\{\omega_n^{(i)}\right\}_{i=1}^{N}$, such that

$$p\left(z_{0:n} \mid y_{0:n}\right) \approx \sum_{i=1}^{N} \omega_n^{(i)} \delta\left(z_{0:n} - z_{0:n}^{(i)}\right) \tag{21}$$

where δ is the Dirac delta.

In practice, it is not possible to efficiently sample from the true posterior $p\left(z_{0:n} \mid y_{0:n}\right)$, given that it is seldom known exactly. To overcome this problem, a Sequential Importance Sampling (SIS) approach can be adopted. To this end, an importance density PDF $q\left(z_{0:n} \mid y_{0:n}\right)$ defined over a support region including that of the true posterior PDF can be conveniently defined so that samples can be efficiently generated from it. Thus, to compensate for the difference between the importance density and the true posterior density, the unnormalized particle weights are computed as:

$$\hat{\omega}_n^{(i)} = \frac{p\left(z_{0:n}^{(i)} \mid y_{0:n}\right)}{q\left(z_{0:n}^{(i)} \mid y_{0:n}\right)} \tag{22}$$

where $\omega_n^{(i)} = \dfrac{\hat{\omega}_n^{(i)}}{\sum_{i=1}^{N} \hat{\omega}_n^{(i)}}$, $i = 1,\ldots,N$.

It follows that the choice of the importance density is crucial for the particle filter algorithm, so that a bad election may lead to a poor algorithm performance (i.e. larger variances of the particle-based estimation). There is a vast literature dealing with optimal choice of importance density (Arulampalam *et al.*, 2002; Doucet *et al.*, 2001) however in most of the practical applications the importance density is conveniently chosen as $q\left(z_{0:n} \mid y_{0:n}\right) = q\left(z_{0:n} \mid y_{0:n-1}\right)$, so that it can be factorized as $q\left(z_{0:n} \mid y_{0:n-1}\right) = q\left(z_n \mid z_{n-1}\right) q\left(z_{0:n-1} \mid y_{0:n-1}\right)$ (Arulampalam *et al.*, 2002). Thus, by substituting Equation (10) into Equation (22), the unnormalized weight for the i^{th} particle at time n can be rewritten as:

$$\hat{\omega}_n^{(i)} \propto \underbrace{\frac{p\left(z_{0:n-1}^{(i)} \mid y_{0:n-1}\right)}{q\left(z_{0:n-1}^{(i)} \mid y_{0:n-1}\right)}}_{\omega_{n-1}^{(i)}} \frac{p\left(z_n^{(i)} \mid z_{n-1}^{(i)}\right) p\left(y_n \mid z_n^{(i)}\right)}{q\left(z_n^{(i)} \mid z_{n-1}^{(i)}\right)} \tag{23}$$

Typically, the PDF $q\left(z_n \mid z_{n-1}\right)$ in Equation (23) is chosen to coincide with the state transition equation $p\left(z_n \mid z_{n-1}\right)$ (Gordon *et al.*, 1993; Tanizaki & Mariano, 1998) since it is easy to evaluate. In this case the last equation simplifies to

$$\hat{\omega}_n^{(i)} \propto \omega_{n-1}^{(i)} p\left(y_n \mid z_n^{(i)}\right) \tag{24}$$

and the resulting algorithm is commonly known as "bootstrap filter", after (Gordon *et al.*, 1993).

A well-known and unavoidable problem when using particle filters based on SIS is the weight degeneracy, by which the normalized probability mass tends to concentrate over a decreasing number of particles as long as the number of iterations increases (Arulampalam *et al.*, 2002; Cappé *et al.*, 2007). A common solution is to introduce a resampling step whenever a significant degeneracy is observed (e.g., by quantifying the effective sample size, ESS, (Kong *et al.*, 1994)). By the resampling, the particles with higher weights are replicated while those with low weights are removed, using the normalized weights as probabilities of selection. After the resampling step, the normalized importance weights are reset to $1/N$. A pseudocode implementation for a SIS particle filter with resampling and parameter regeneration is provided in Algorithm 1.

Finally, given the current state estimation based on particle filters, a filtered estimation of the predictive PDF $p(z_{n+\ell} \mid y_{0:n})$ can be obtained by replacing $p\left(z_n \mid y_{0:n}\right)$ in Equation (16) by its particle-filter approximation (as a marginal of the updating PDF in Equation 21) as follows:

$$\begin{aligned} p\left(z_{n+\ell} \mid y_{0:n}\right) \approx & \int_{\mathcal{Z}} \prod_{l=n+1}^{n+\ell} p\left(z_l \mid z_{l-1}\right) \sum_{i=1}^{N} \omega_n^{(i)} \delta\left(z_{0:n} - z_{0:n}^{(i)}\right) dz_{n:n+\ell-1} \\ = & \sum_{i=1}^{N} \omega_n^{(i)} \int_{\mathcal{Z}} p\left(z_{n+1} \mid z_n^{(i)}\right) \prod_{l=n+2}^{n+\ell} p\left(z_l \mid z_{l-1}\right) dz_{\boldsymbol{n}+1:n+\ell-1} \end{aligned} \tag{25}$$

Note that the last equation cannot be solved analytically, however it can be sampled by drawing one conditional sample trajectory $z_{n+1:n+\ell}^{(i)} = \left\{z_{n+1}^{(i)}, z_{n+2}^{(i)}, \ldots, z_{n+\ell}^{(i)}\right\}$ from each of the N multidimensional integrals appearing in Equation (25). This can be readily achieved by conditional sampling, using the one-step transition equation defined in Equation (11), i.e.: first sample $z_{n+1}^{(i)}$ using the aforementioned state transition equation conditional on a sample from the filtered state $z_n^{(i)}$, i.e., $z_{n+1}^{(i)} \sim p\left(z_{n+1} \mid z_n^{(i)}\right)$; then sample the succeeding state conditional on the previous sample, i.e. $z_{n+2}^{(i)} \sim p\left(z_{n+2} \mid z_{n+1}^{(i)}\right)$; finally, repeat the same process until the target time $n+\ell$ is reached. Finally, an estimate of the $\ell-$ step predictive ahead PDF can be expressed as

$$p\left(z_{n+\ell} \mid y_{0:n}\right) \approx \sum_{i=1}^{N} \omega_n^{(i)} \delta\left(z_{n+\ell} - z_{n+\ell}^{(i)}\right) \tag{26}$$

where $\omega_n^{(i)}$ is the weight of i^{th} particle at time of prediction n.

Algorithm 1. SIS particle filter with parameter adaptation

1: At $n = 0$

2: Generate $\left\{x_0^{(i)}, \theta_0^{(i)}\right\}_{i=1}^{N}$, sampling from prior PDFs $p(x_0)$ and $p(\theta)$, respectively.

3: Assign the initial weights: $\left\{\omega_0^{(i)} = 1/N\right\}_{i=1}^{N}$

4: At $n \geq 1$

5: Set initial covariance for artificial dynamics: $\Sigma_{\xi_0} = diag\left(\sigma_{\xi_{0,1}}^2, \ldots, \sigma_{\xi_{0,n_\theta}}^2\right)$

6: **for** $i = 1$ to N

7: Sample from Eq.: $\theta_n^{(i)} \sim p\left(\theta \mid \theta_{n-1}^{(i)}\right)$

8: Sample from Eq.: $x_n^{(i)} \sim p\left(x_n \mid x_{n-1}^{(i)}, \theta_n^{(i)}\right)$

9: Set $z_n^{(i)} = \left(x_n^{(i)}, \theta_n^{(i)}\right)$ and $z_{0:n}^{(i)} = \left\{z_{0:n-1}^{(i)}, z_n^{(i)}\right\}$

10: Update weights according to Eq.: $\hat{\omega}_n^{(i)} \propto \omega_{n-1}^{(i)} p\left(y_n \mid z_n^{(i)}\right)$

11: **end for**

12: **for** $i = 1$ to N

13: Normalize $\omega_n^{(i)} \leftarrow \hat{\omega}_n^{(i)} \Big/ \sum_{j=1}^{N} \hat{\omega}_n^{(j)}$

14: **end for**

15: **for** $j = 1$ to n_θ

16: Sample $\left\{\tilde{\theta}_{n,j}^{(k)}\right\}_{k=1}^{K} \sim p\left(\theta_{n,j} \mid y_{0:n}\right) \approx \sum_{i=1}^{N} \omega_n^{(i)} \delta\left(\theta_{n,j} - \theta_{n,j}^{(i)}\right)$

continued on following page

Algorithm 1. Continued

17: Compute $\mathrm{RMAD}\left(\theta_{n,j}\right)$ according to Eq.

18: Update variance of random walk: $\sigma^2_{\xi_{n,j}} = \sigma^2_{\xi_{n-1,j}} \left(1 - P^*_j \dfrac{\mathrm{RMAD}\left(\theta_{n,j}\right) - RMAD^*_j}{\mathrm{RMAD}\left(\theta_{n,j}\right)}\right)$

19: **end for**

20: set $\Sigma_{\xi_n} = diag\left(\sigma^2_{\xi_{n,1}}, \cdots, \sigma^2_{\xi_{n,n_\theta}}\right)$

21: **if** EES $< N_T$

22: $\left\{z^{(i)}_n, 1/N\right\}_{i=1}^{N} \leftarrow \mathrm{Resample}\left\{z^{(i)}_n, \omega^{(i)}_n\right\}_{i=1}^{N}$

23: **end if**

Having estimated the current state of the system and the future state $\ell -$ steps ahead, Algorithm 2 can be used for predicting the RUL and EOL of the system. Using the updated weights of the particles at time of prediction $n = n_p$, a probabilistic estimation of the EOL can be obtained as:

$$p\left(EOL_{n_p} \mid y_{0:n_p}\right) \approx \sum_{i=1}^{N} \omega^{(i)}_{n_p} \delta\left(EOL_{n_p} - EOL^{(i)}_{n_p}\right) \tag{27}$$

where $\omega^{(i)}_{n_p}$ is the normalized weight of the i^{th} particle at time of prediction n_p. From the EOL estimation of the i^{th} particle, denoted as $EOL^{(i)}_{n_p}$, the remaining useful life for that particle can be readily obtained as $RUL^{(i)}_{n_p} = EOL^{(i)}_{n_p} - n_p$. By adopting the same normalized weights than those used for EOL estimation, a probability-based estimation of RUL can be obtained as:

$$p\left(RUL_{n_p} \mid y_{0:n_p}\right) \approx \sum_{i=1}^{N} \omega^{(i)}_{n_p} \delta\left(RUL_{n_p} - RUL^{(i)}_{n_p}\right) \tag{28}$$

The details of the method for EOL and RUL prediction are summarized in Algorithm 2.

PROGNOSTICS EXAMPLE ON COMPOSITE MATERIALS

The proposed framework is exemplified using SHM data obtained from a set of carefully designed run-to-failure fatigue experiments in cross-ply graphite-epoxy laminates. This example is motivated by the

Algorithm 2. EOL and RUL prediction

Inputs: $\left\{\left(x_{n_p}^{(i)}, \theta_{n_p}^{(i)}\right), \omega_{n_p}^{(i)}\right\}_{i=1}^{N}$

Outputs: $\left\{EOL_{n_p}^{(i)}, RUL_{n_p}^{(i)}, \omega_{n_p}^{(i)}\right\}_{i=1}^{N}$

1: $n \leftarrow n_p$

2: **for** $i = 1$ to N

3: **while** $T_{EOL}\left(x_n^{(i)}, \theta_n^{(i)}\right) = 0$

4: Sample: $\theta_{n+1}^{(i)} \sim p\left(\theta_{n+1} \mid \theta_n^{(i)}\right)$;

5: Sample: $x_{n+1}^{(i)} \sim p\left(x_{n+1} \mid x_n^{(i)}, \theta_{n+1}^{(i)}\right)$;

6: $\left(x_n^{(i)}, \theta_n^{(i)}\right) \leftarrow \left(x_{n+1}^{(i)}, \theta_{n+1}^{(i)}\right)$

7: $n \leftarrow n + 1$

8: **end while**

9: $EOL_{n_p}^{(i)} \leftarrow n$

10: $RUL_{n_p}^{(i)} = EOL_{n_p}^{(i)} - n$

11: **end for**

high dispersion that can be observed when degradation data are obtained from fatigue tests in composite materials, even for tests of nominally identical specimens. This highlights the need of integrating the SHM system within a Bayesian prognostic framework to deal with RUL prediction along with its quantified uncertainty. In this exercise, Torayca T700G unidirectional carbon pre-preg material was used for $15.24\ [\mathrm{cm}] \times 25.4\ [\mathrm{cm}]$ coupons with dog-bone geometry and $\left[0_2 / 90_4\right]_s$ stacking sequence, whose mechanical properties are listed in Table 1 (at this point, see only the nominal values in the 3rd column). A notch ($5.1\ [\mathrm{mm}] \times 19.3\ [\mathrm{mm}]$) was created in these coupons to induce damage modes others than matrix-cracks, such as delamination, thereby introducing additional sources of uncertainty and then demonstrating the proposed framework under more realistic conditions.

Description of Experiment Set-Up and SHM Data

SHM data for this numerical example consist of periodically measurements for laminate stiffness reduction, as a measure of macro-scale manifestation of damage, along with micro-crack density and delamination area, as micro-scale manifestation of damage. Fatigue tests were conducted under load-controlled tension-tension cyclic loading with a maximum applied load of $31.13\ [\mathrm{KN}]$, a frequency $f = 5\ [\mathrm{Hz}]$, and a stress ratio $R = 0.14$ (relation between the minimum and maximum stress for each fatigue cycle). Monitoring data were collected from a network of 12 piezoelectric (PZT) sensors SMART Layer® from Acellent Technologies Inc. using Lamb wave signals and three triaxial strain-gages. Additionally, periodic X-rays were taken to visualize and characterize subsurface damage features, in particular, the micro-cracks density. This information was then used to develop a mapping between PZT raw signals and micro-cracks density, as reported in Larrosa and Chang (Larrosa & Chang, 2012). More details about these tests are reported in the Composite dataset, NASA Ames Prognostics Data Repository (Saxena *et al.*, 2013). Damage data used in this example correspond to laminate L1S19 in (Saxena *et al.*, 2013).

Table 1. Nominal values and prior uncertainty for main parameters used in calculations; parameters selected for sequential updating are identified in parentheses. The nominal values for fitting and error parameters have been defined through initial fitting tests. See Table 2 for nomenclature description.

Type	Parameter	Nominal Value	Units	Prior PDF
Mechanical	E_1 (θ_1)	127.55	GPa	LogN(ln(127.55), 0.1)
	E_2 (θ_2)	8.41	GPa	LogN(ln(8.41), 0.1)
	G_{12}	6.20	GPa	LogN(ln(6.20), 0.1)
	ν_{12}	0.31	--	LogN(ln(0.31), 0.1)
	G_{23}	2.82	GPa	LogN(ln(2.82), 0.1)
	d (θ_3)	$1.5 \cdot 10^{-4}$	m	LogN(ln($1.5 \cdot 10^{-4}$), 0.1)
Fitting	α (θ_4)	1.8	--	LogN(ln(1.8), 0.2)
	A	10^{-4}	--	LogN(ln(10^{-4}), 0.2)
Error	σ_{v1} (θ_5)	--	cracks/(m × cycle)	U(0.5,1.5)
	σ_{v2} (θ_6)	--	--	U(0.001,0.003)

Damage Model

The rate of change of internal damage per cycle can be evaluated by the modified Paris' law (Nairn & Hu, 1992) as follows:

$$\frac{d\rho}{dn} = A(\Delta G)^{\alpha} \tag{29}$$

where ρ is the matrix micro-crack density, and α and A are fitting parameters. The term ΔG is the increment in energy release rate G evaluated for the maximum and minimum stress in the cyclic load series: $\Delta G = G\Big|_{\sigma_{max}} - G\Big|_{\sigma_{min}}$. For a given axial tension σ_x, the energy released by the formation of a new crack between two existing cracks can be calculated using the following expression:

$$G\Big|_{\sigma_x} = \frac{\sigma_x^2 h}{2\rho t_{90}}\left(\frac{1}{E_x^*\left(2\rho\right)} - \frac{1}{E_x^*\left(\rho\right)}\right) \tag{30}$$

where h and t_{90} are the laminate and 90º-sublaminate half-thickness, respectively. The term $E_x^*(\rho)$, as a function of crack density ρ, is the effective laminate Young's modulus due to the current damage state. Several micro-damage mechanic models from the literature (Talreja & Singh, 2012) can be adopted to evaluate $E_x^*(\rho)$, e.g. *shear-lag models* (Garrett & Bailey, 1977; Highsmith & Reifsnider, 1982) *variational models* (Hashin, 1985), and *crack opening displacement* based models (Gudmundson & Weilin, 1993; Lundmark & Varna, 2005), among others. The shear-lag approach is adopted in this work for being simpler and well suited for symmetric cross-ply laminates (J. Chiachio *et al.*, 2015), which is the laminate type used for this study. Following this approach, $E_x^*(\rho)$ can be obtained as (Joffe & Varna, 1999):

$$E_x^* = \frac{E_{x,0}}{1 + a\,\frac{1}{2\bar{l}}\,R\left(\bar{l}\right)} \tag{31}$$

In the last equation, $E_{x,0}$ is the initial (undamaged) longitudinal Young's modulus of the laminate; $\bar{l}$ is the half crack-spacing normalized by the 90° sub-laminate thickness, i.e., $\bar{l} = l \big/ \rho t_{90}$ where $l = 1 \big/ 2\rho$; and a is a known function of the laminate mechanical and geometrical properties, defined as follows:

$$a = \frac{E_2 t_{90}}{E_1 t_0}\left(h\,\frac{\nu_{12}\cdot\left(1-\nu_{12}\right)}{t_{90} + t_0\,\frac{E_2}{E_1}}\right)\frac{1-\nu_{12}^2}{1-\nu_{12}^2\,\frac{E_2}{E_1}} \tag{32}$$

Regarding the initial Young's modulus of the laminate $E_{x,0}$, it can be approximated for this example using a simple rule of mixtures as

$$E_{x,0} = \frac{t_0 E_1 + t_{90} E_2}{t_0 + t_{90}} \tag{33}$$

The function $R(\bar{l})$ in Equation (31) is known as the *average stress perturbation function* (Joffe & Varna, 1999), and it is defined as:

$$R\left(\bar{l}\right) = \frac{2}{\xi}\tanh\left(\xi\bar{l}\right) \tag{34}$$

where

$$\xi^2 = G_{23}\left(\frac{1}{E_2} + \frac{1}{\lambda E_1}\right) \tag{35}$$

and $\lambda = h_0 \big/ h_{90}$. For the sake of clarity, a description of the terms involved in Equations (32) and (35) is provided in Table 2.

At this standpoint, it is easy to understand that a closed-form solution for the resulting Paris' Law equation is difficult to obtain. This is due to the complexity of the expression for ΔG, which involves the underlying micro-damage mechanics model for the computation of $E_x^*(\rho)$. To overcome this draw-

Table 2. Nomenclature description for main geometric and mechanical parameters

Level	Parameter	Description
Laminate	E_x	Longitudinal Yong's modulus
	E_x*	Effective long. Young's modulus
	h	Laminate half-thickness
	t_{90}	90º-sublaminate half-thickness
	t_0	0º-sublaminate thickness
Ply	E_1	Longitudinal Young's modulus
	E_2	Transverse Young's modulus
	ν_{12}	In-plane Poisson ratio
	G_{12}	In-plane shear modulus
	G_{23}	Out-of-plane shear modulus
	d	Ply thickness

back, the resulting differential equation in (29) can be solved by approximating the derivative using "unit-cycle' finite differences by assuming that damage evolves cycle-to-cycle as:

$$\rho_n = \rho_{n-1} + A\left(\Delta G\left(\rho_{n-1}\right)\right)^{\alpha} \tag{36}$$

where ρ_n denotes the matrix micro-cracks density at cycle n.

Stochastic Embedding of Damage Models

In this section, the PF-based prognostic framework presented above is specialized to the fatigue damage modeling approach explained in the last section. To this end, let consider that the progression of damage is studied by focusing on the matrix-cracks density ρ_n, and the normalized effective stiffness, defined as $D_n = E_x^* / E_{x,0}$, describing a joint state transition equation of two components $g = \left(g_1, g_2\right)$ as follows:

$$\begin{aligned} x_{1,n} &= \rho_n = \underbrace{g_1\left(\rho_{n-1}, u_n, \theta\right)}_{\text{Eq. 36}} + v_{1,n} \\ x_{2,n} &= D_n = \underbrace{g_2\left(\rho_n, \boldsymbol{u}_n, \theta\right)}_{\text{Eq. 31}} + v_{2,n} \end{aligned} \tag{37}$$

where $x_n = \left(x_{1,n}, x_{2,n}\right) \in \mathbb{R}^2$ is the system response at cycle *n*, and $v_n = \left(v_{1,n}, v_{2,n}\right) \in \mathbb{R}^2$ is the model error vector for the overall system. Subscripts 1 and 2 correspond to each of the damage subsystems, namely, matrix-crack density and normalized effective stiffness, respectively. A key concept here is the consideration of model errors $v_{1,n}$ and $v_{2,n}$ as stochastically independent, even though the models corresponding to the damage subsystems g_1 and g_2 are mathematically related, as shown in Equation (37). It follows that the covariance operator Σ_{v_n} in Equation (8) is a diagonal matrix, i.e., $\Sigma_{v_n} = diag\left(\sigma_{v_{1,n}}, \sigma_{v_{2,n}}\right)$, where $\sigma_{v_{1,n}}$ and $\sigma_{v_{2,n}}$ are the corresponding standard deviations of errors $v_{1,n}$ and $v_{2,n}$ respectively. Therefore, the state transition equation of the overall system can be readily expressed as a product of univariate Gaussians, as:

$$p\left(x_n \mid x_{n-1}, \theta\right) = p\left(D_n \mid \rho_n, \theta\right) p\left(\rho_n \mid \rho_{n-1}, \theta\right) \tag{38}$$

where

$$\begin{aligned} p\left(\rho_n \mid \rho_{n-1}, \theta\right) &= \frac{1}{\sqrt{2\pi}\sigma_{v_{n,1}}} \exp\left(-\frac{\left(\rho_n - g_1\left(\rho_{n-1}, \theta\right)\right)^2}{2\sigma_{v_{n,1}}^2}\right) \\ p\left(D_n \mid \rho_n, \theta\right) &= \frac{1}{\sqrt{2\pi}\sigma_{v_{n,2}}} \exp\left(-\frac{\left(D_n - g_2\left(\rho_n, \theta\right)\right)^2}{2\sigma_{v_{n,2}}^2}\right) \end{aligned} \tag{39}$$

In the last equations the model parameters θ are selected among the complete set of mechanical and geometrical parameters describing Equations (29) to (35) (see Table 1) through a Global Sensitivity Analysis following the methodology proposed by (Saltelli *et al.*, 2008). The ply properties $\{E_1, E_2, t\}$ together with the fitting constant α emerged as sensitive parameters to model output uncertainty (J. Chiachio *et al.*, 2015). To the last cited selection, the standard deviations of the model errors $v_{1,n}$ and $v_{2,n}$ are added since they are uncertain a priori, resulting in $\theta = \left(\alpha, E_1, E_2, t, \sigma_{v_{1,n}}, \sigma_{v_{2,n}}\right) \in \mathbb{R}^6$. The rest of parameters are fixed at any point within their range of variation, (e.g. the mean value) without significantly influencing the output uncertainty.

To allow the incorporation of SHM measurement to the stochastic system, the following measurement equation is considered:

$$y_n = x_n + w_n \tag{40}$$

where $y_n = \left(y_{1,n}, y_{2,n}\right) \equiv \left(\hat{\rho}_n, \hat{D}_n\right) \in \mathbb{R}^2$ are measurements for both matrix-cracks density and normalized effective stiffness respectively, and $w_n = \left(w_{1,n}, w_{2,n}\right) \in \mathbb{R}^2$ is the vector of measurement errors. As stated before, the PMIE is used to choose w_n as Gaussian PDF with covariance matrix Σ_{w_n}. Thus, the *measurement equation* defined in Equation (40) can be expressed in probabilistic terms as:

$$p(y_n \mid x_n) = \left((2\pi)^{n_y} \mid \Sigma_{w_n} \mid\right)^{-\frac{1}{2}} \exp\left(-\frac{1}{2}\left(y_n - x_n\right)^T \Sigma_{w_n}^{-1}\left(y_n - x_n\right)\right) \tag{41}$$

Since the measurements of each subsystem (micro-cracks and stiffness loss) are considered as stochastically independent, then $\Sigma_{w_n} = diag\left(\sigma_{w_{1,n}}, \sigma_{w_{2,n}}\right)$. Here $\sigma_{w_{1,n}}$ and $\sigma_{w_{2,n}}$ are the standard deviation of the corresponding measurement errors $w_{1,n}$ and $w_{2,n}$ respectively. Thus, the measurement equation defined in (41) can be readily expressed as:

$$p\left(y_n \mid x_n\right) = p\left(\hat{\rho}_n \mid \rho_n\right) p\left(\hat{D}_n \mid D_n\right) \tag{42}$$

where

$$\begin{aligned} p\left(\hat{\rho}_n \mid \rho_n\right) &= \frac{1}{\sqrt{2\pi}\sigma_{w_{1,n}}} \exp\left(-\frac{\left(\hat{\rho}_n - \rho_n\right)^2}{2\sigma_{w_{1,n}}^2}\right) \\ p\left(\hat{D}_n \mid D_n\right) &= \frac{1}{\sqrt{2\pi}\sigma_{w_{2,n}}} \exp\left(-\frac{\left(\hat{D}_n - D_n\right)^2}{2\sigma_{w_{2,n}}^2}\right) \end{aligned} \tag{43}$$

Finally, by substituting the Equation (42) into (24), the formula for updating the particle weights leads to the next expression:

$$\omega_n^{(i)} \propto \omega_{n-1}^{(i)} p\left(\hat{\rho}_n \mid \rho_n^{(i)}\right) p\left(\hat{D}_n \mid D_n^{(i)}\right) \tag{44}$$

Results for RUL Prediction

This section presents RUL prediction results on the composite fatigue example and also illustrates the use of prognostics metrics for prediction performance evaluation. As fatigue data become available, the prognostic algorithm makes predictions of when micro-cracks density and the normalized effective stiffness reach their respective thresholds, defining the EOL and RUL for this experiment.

Every time new data arrive, the damage variables $x_n = \left(\rho_n, D_n\right)$ together with model parameters θ_n are updated using Algorithm 1 with $N = 5000$ particles. The scaling variables $RMAD_j^*$ and P_j^* (see Algorithm 1) are fixed to $0.3RMAD_{0,j}$ and 0.001, respectively, where $RMAD_{0,j}$ is calculated according to Equation (15) using samples from the marginal prior $p(\theta_j)$, $j = 1,\ldots,6$. The prior PDFs of model parameters are specified in Table 1. The diagonal elements of the covariance matrix $\Sigma_{\xi_{0,j}}$ (recall Equation (13)) are appropriately selected through some initial test runs and set at 0.5% of the 5th-95th inter-percentile range of the prior PDFs for each of the j^{th} component of θ. For this example, the systematic importance resampling (SIR) version of the SIS algorithm is adopted whereby the resampling step is run every time new data are collected, hence $ESS = N$. Damage states are initialized at $x_0 = \left(\rho_0, D_0\right)$, being $\rho_0 = 0.1\ \left[cracks/mm\right]$ and $D_0 = 1$ (dimensionless). The standard deviation of the measurement error parameters are set to $\sigma_{w_{1,n}} = 0.05\ \left[cracks/mm\right]$ and $\sigma_{w_{2,n}} = 0.01$, taking them as known. At each time n, the updated damage states are further propagated into the future using the models to compute the remaining useful life of the laminate, calculated as $RUL_n = EOL_n - n$, following the methodology described above. The region of acceptable performance is defined in this example as $\mathcal{A} \triangleq \left\{(\rho, D) \in [0, 0.42] \times [0.88, 1]\right\} \subset \mathbb{R}^2$, where ρ is expressed in $\left[cracks/mm\right]$ and D is dimensionless.

Figure 7 shows the results for damage state estimation and multi-step ahead prediction at fatigue cycles $n = \{1, 3, 8\} \times 10^4$ for both, micro-cracks density and relative stiffness loss. While predictions are generally updated at regular intervals, for the sake of conciseness and clarity only three predictions are presented here. The solid black markers indicate the measurement data available until time of prediction n. For comparison purposes, the upcoming data are also represented using hollow markers. The multi-step ahead predictions for both damage features are shown in solid lines. Additionally, two credibility interval ranges, 25%-75% (dark dashed lines) and 5%-95% (light dashed lines), are included to show the uncertainty in the predicted estimates. Since predictions are updated at regular intervals, the uncertainty reduction is clearly revealed by comparing the credibility intervals at increasing prediction times.

The results for remaining useful life are plotted in Figure 8, where RUL predictions made at different times (about every 10,000 cycles) are plotted with corresponding uncertainties represented as error bars.

Figure 7. Example results for sequential state estimation and multi-step ahead prediction made at prediction times $n = \{1, 3, 8\} \times 10^4$

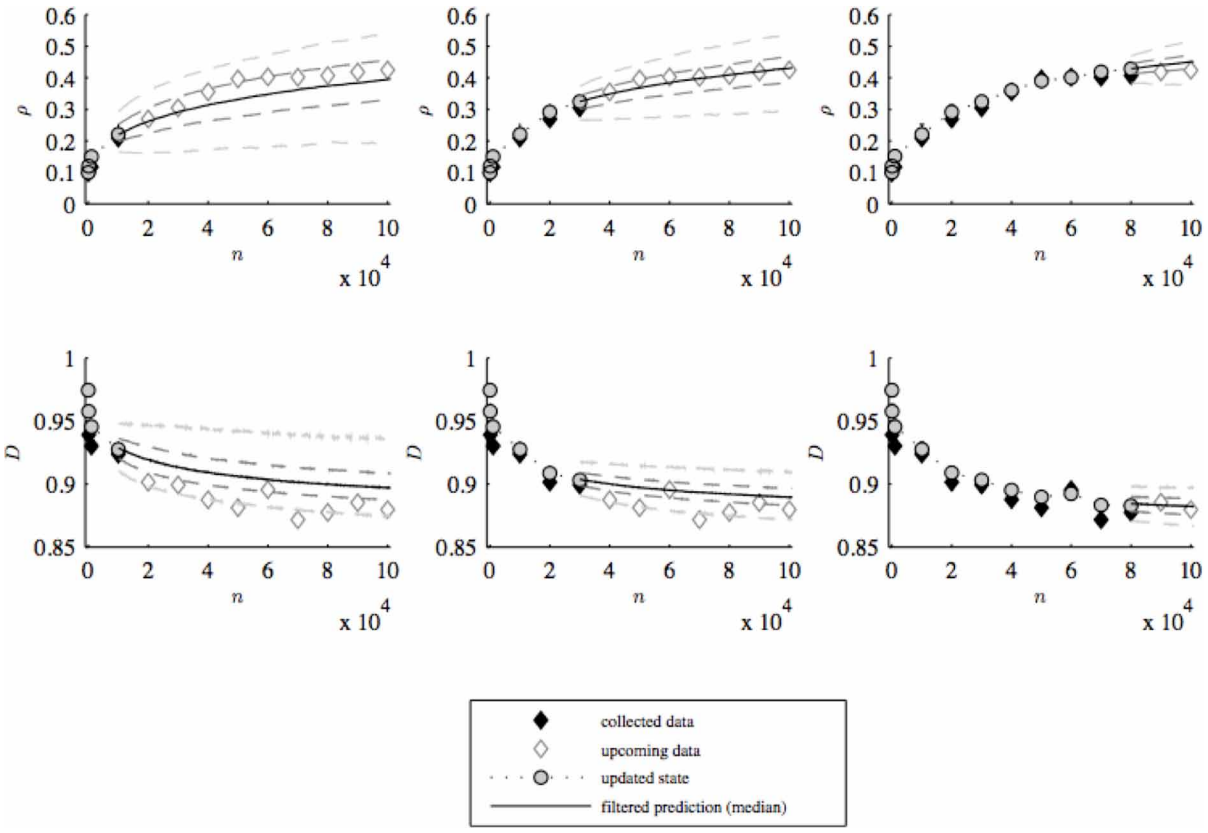

Two cones of accuracy at 10% and 20% of true RUL, denoted as RUL*, are included to interpret performance with regards to prediction accuracy and precision.

Observe that the RUL prediction is significantly inaccurate for the first few predictions during the early stages of the fatigue process, which is attributed to the time lapse required for SHM data to train model parameters. From this period, not only the prediction precision clearly improves with time (values closer to RUL* line), but also the prediction uncertainty gradually tends to diminish. This visualization allows assessment of how prediction performance changes over time in terms of *correctness* (accuracy and precision). Also, by assessing how quickly performance converges within desired accuracy levels one can estimate the prediction horizon, as defined in Fundamentals. In particular for this example, the PH for 0.2 as α-accuracy is PH=$8 \cdot 10^4$-$1 \cdot 10^3$=$7.9 \cdot 10^4$ cycles.

Furthermore, the error bars and their pattern of shrinkage contribute to the confidence in predictions vis-à-vis and their usage in decision making. It is also noteworthy in Figure 8 that accuracy seems to depart from true RUL at the final stages of the fatigue process, which indicates that the model and its variance structure do not fully capture the damage dynamics towards the end of the damage process. Such behavior has been previously reported in (Saxena, Celaya, *et al.*, 2010a) and may be related to the difficulty of obtaining adequate amount of measurements to account for behaviors when the damage process has reached asymptotic growth behavior.

Figure 8. Using RUL vs. time plot to assess Remaining Useful Life prediction performance for composites under fatigue aging

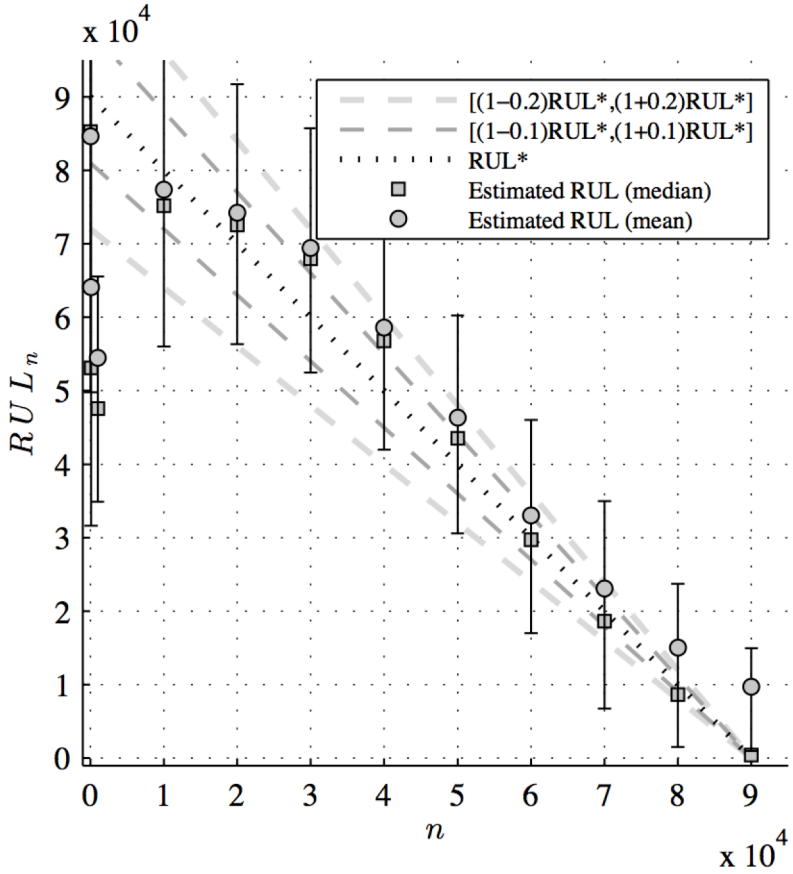

CONCLUSION

This chapter presented a generic framework for prognostics and remaining useful life prediction. First, an architecture for prognostics was developed; in this architecture, prognostics was broken down into the three important problems of state estimation, future state prediction, and remaining useful life prediction. Stochastic state-space system models were used to depict the degradation of system health that was in turn represented using the states of the system. These states were estimated using output measurements and the estimated states were used to forecast state values and hence, the health of the system. The end of life was defined using a multi-dimensional threshold function and the time-instant at which the system reaches end of life was calculated.

A key feature of the above methodology was a systematic treatment of the various sources of uncertainty. Since prognostics deals with the prediction of future events, it is important to understand that it is almost impossible to make precise predictions due to the various uncertainties that cloud the future. To being with, the interpretation of uncertainty was discussed in detail. The traditional frequentist approach is not suitable for understanding uncertainty in condition-based prognostics and it is necessary to adopt a subjective approach for interpreting uncertainty in this context. Therefore, a Bayesian approach

that is based on the concept of subjective probability is extremely suitable for investigating uncertainty in prognostics.

The various sources of uncertainty in prognostics include system inputs (loading, environmental, operational conditions), system parameters, state-space models, etc. As a result of these sources of uncertainty, the state estimates, future state predictions, and the remaining useful life are all uncertain. It is necessary to understand that these quantities are simply dependent on the different sources of uncertainty and hence, it is important to systematically quantify the effect of the various sources of uncertainty on prognostics and remaining useful life prediction. This was accomplished through the use of Bayesian state estimation that can compute the probability distribution of the system states by accounting the different sources of uncertainty. Then, it was illustrated that, in order to accurately calculate the probability distribution of remaining useful life, the prediction of remaining useful life needs to be posed as an uncertainty propagation problem that can be solved using a variety of statistical techniques. Some of these methods were briefly discussed, and algorithms were provided for both state estimation and RUL prediction.

REFERENCES

Arulampalam, M. S., Maskell, S., Gordon, N., & Clapp, T. (2002). A tutorial on particle filters for online nonlinear/non-Gaussian Bayesian tracking. *Signal Processing*. *IEEE Transactions on*, *50*(2), 174–188. doi:10.1109/78.978374

Au, S. K., & Beck, J. L. (2001). Estimation of small failure probabilities in high dimensions by Subset Simulation. *Probabilistic Engineering Mechanics*, *16*(4), 263–277. doi:10.1016/S0266-8920(01)00019-4

Bucher, C. G. (1988). Adaptive sampling—an iterative fast Monte Carlo procedure. *Structural Safety*, *5*(2), 119–126. doi:10.1016/0167-4730(88)90020-3

Caflisch, R. E. (1998). Monte carlo and quasi-monte carlo methods. *Acta Numerica*, *1998*, 1–49. doi:10.1017/S0962492900002804

Cappé, O., Godsill, S. J., & Moulines, E. (2007). An overview of existing methods and recent advances in sequential Monte Carlo. *Proceedings of the IEEE*, *95*(5), 899–924. doi:10.1109/JPROC.2007.893250

Celaya, J., Saxena, A., & Goebel, K. (2012). *Uncertainty Representation and Interpretation in Model-based Prognostics Algorithms based on Kalman Filter Estimation*. Paper presented at the Proceedings of the Annual Conference of the PHM Society.

Chang, F.-K., Markmiller, J. F. C., Ihn, J.-B., & Cheng, K. Y. (2007). A Potential Link from Damage Diagnostics to Health Prognostics of Composites Through Built-in Sensors. *Transaction of the ASME, 129*(December). doi:10.1115/1.2730530

Chiachio, J., Chiachio, M., Saxena, A., Sankararaman, S., Rus, G., & Goebel, K. (2015). Bayesian Model Selection and Parameter Estimation for Fatigue Damage Progression Models in Composites. *International Journal of Fatigue*, *70*, 361–373. doi:10.1016/j.ijfatigue.2014.08.003

Chiachio, M., Chiachio, J., Saxena, A., & Goebel, K. (2014). An efficient simulation framework for prognostics of asymptotic processes- a case study in composite materials. *2nd European Conference of the Prognostics and Health Management Society, Nantes, France2014. EPHM 20141*.

Daigle, M., Saxena, A., & Goebel, K. (2012). *An Efficient Deterministic Approach to Model-based Prediction Uncertainty Estimation*. Paper presented at the Annual Conference of the Prognostics and Health Management Society.

Daigle, M. J., & Goebel, K. (2013). Model-based prognostics with concurrent damage progression processes. *Systems, Man, and Cybernetics: Systems. IEEE Transactions on*, *43*(3), 535–546.

Der Kiureghian, A., Lin, H.-Z., & Hwang, S.-J. (1987). Second-order reliability approximations. *Journal of Engineering Mechanics*, *113*(8), 1208–1225. doi:10.1061/(ASCE)0733-9399(1987)113:8(1208)

Dolinski, K. (1983). First-order second-moment approximation in reliability of structural systems: Critical review and alternative approach. *Structural Safety*, *1*(3), 211–231. doi:10.1016/0167-4730(82)90027-3

Doucet, A., De Freitas, N., & Gordon, N. (2001). *Sequential Monte Carlo methods in practice*. Springer Verlag. doi:10.1007/978-1-4757-3437-9

Dwight, R. P., & Han, Z.-H. (2009). *Efficient uncertainty quantification using gradient-enhanced kriging*. Paper presented at the 11th AIAA Non-Deterministic Approaches Conference, Reston, VA.

Engel, S. J., Gilmartin, B. J., Bongort, K., & Hess, A. (2000). *Prognostics, the real issues involved with predicting life remaining*. Paper presented at the Aerospace Conference Proceedings. IEEE. doi:10.1109/AERO.2000.877920

Farrar, C. R., & Lieven, N. A. (2007). Damage prognosis: the future of structural health monitoring. *Philosophical Transactions of the Royal Society A: Mathematical, Physical and Engineering Sciences, 365*(1851), 623-632.

Garrett, K., & Bailey, J. (1977). Multiple transverse fracture in Latex translation cross-ply laminates of a glass fibre-reinforced polyester. *Journal of Materials Science*, *12*(1), 157–168. doi:10.1007/BF00738481

Glynn, P. W., & Iglehart, D. L. (1989). Importance sampling for stochastic simulations. *Management Science*, *35*(11), 1367–1392. doi:10.1287/mnsc.35.11.1367

Goebel, K. (2014). PHM Design Process. NASA Ames Research Center.

Gordon, N., Salmond, D., & Smith, A. (1993). Novel approach to nonlinear/non-Gaussian Bayesian state estimation. *IEEE-Proceedings-F*, *140*, 107–113.

Gudmundson, P., & Weilin, Z. (1993). An analytic model for thermoelastic properties of composite laminates containing transverse matrix cracks. *International Journal of Solids and Structures*, *30*(23), 3211–3231. doi:10.1016/0020-7683(93)90110-S

Haldar, A., & Mahadevan, S. (2000). *Probability, reliability, and statistical methods in engineering design*. John Wiley & Sons, Incorporated.

Hashin, Z. (1985). Analysis of cracked laminates: A variational approach. *Mechanics of Materials*, *4*(2), 121–136. doi:10.1016/0167-6636(85)90011-0

Highsmith, A., & Reifsnider, K. (1982). Stiffness-reduction mechanisms in composite laminates. *Damage in composite materials*. *ASTM Special Technical Publication*, *775*, 103–117.

Hohenbichler, M., & Rackwitz, R. (1983). First-order concepts in system reliability. *Structural Safety*, *1*(3), 177–188. doi:10.1016/0167-4730(82)90024-8

Hohenbichler, M., & Rackwitz, R. (1988). Improvement of second-order reliability estimates by importance sampling. *Journal of Engineering Mechanics*, *114*(12), 2195–2199. doi:10.1061/(ASCE)0733-9399(1988)114:12(2195)

Jaynes, E. T. (1983). *Papers on Probability, Statistics and Statistical physics* (R. D. Rosenkrantz, Ed.). Kluwer Academic Publishers.

Joffe, R., & Varna, J. (1999). Analytical modeling of stiffness reduction in symmetric and balanced laminates due to cracks in 90 layers. *Composites Science and Technology*, *59*(11), 1641–1652. doi:10.1016/S0266-3538(99)00025-1

Kalman, R. E. (1960). A new approach to linear filtering and prediction problems. *Journal of Fluids Engineering*, *82*(1), 35–45.

Karamchandani, A., Bjerager, P., & Cornell, C. (1989). *Adaptive importance sampling*. Paper presented at the International Conference on Structural Safety and Reliability.

Kong, A., Liu, J. S., & Wong, W. H. (1994). Sequential imputations and Bayesian missing data problems. *Journal of the American Statistical Association*, *89*(425), 278–288. doi:10.1080/01621459.1994.10476469

Larrosa, C., & Chang, F. (2012). Real time in-situ damage classification, quantification and diagnosis for composite structures *Proceedings of the 19th International Congress on Sound and Vibration* (Vol. 15).

Liu, J., & West, M. (2001). *Combined Parameter and State Estimation in Simulation-Based Filtering* (pp. 197–223). Sequential Monte Carlo Methods in Practice. doi:10.1007/978-1-4757-3437-9_10

Liu, Y., Mohanty, S., & Chattopadhyay, A. (2010). Condition Based Structural Health Monitoring and Prognosis of Composite Structures under Uniaxial and Biaxial Loading. *Journal of Nondestructive Evaluation*, *29*(3), 181–188. doi:10.1007/s10921-010-0076-2

Loh, W.-L. (1996). On Latin hypercube sampling. *Annals of Statistics*, *24*(5), 2058–2080. doi:10.1214/aos/1069362310

Lundmark, P., & Varna, J. (2005). Constitutive relationships for laminates with ply cracks in in-plane loading. *International Journal of Damage Mechanics*, *14*(3), 235–259. doi:10.1177/1056789505050355

Nairn, J., & Hu, S. (1992). The initiation and growth of delaminations induced by matrix microcracks in laminated composites. *International Journal of Fracture*, *57*(1), 1–24. doi:10.1007/BF00013005

Najm, H. N. (2009). Uncertainty quantification and polynomial chaos techniques in computational fluid dynamics. *Annual Review of Fluid Mechanics*, *41*(1), 35–52. doi:10.1146/annurev.fluid.010908.165248

Orchard, M., Kacprzynski, G., Goebel, K., Saha, B., & Vachtsevanos, G. (2008). *Advances in uncertainty representation and management for particle filtering applied to prognostics*. Paper presented at the Prognostics and Health Management, 2008. PHM 2008. International Conference on. doi:10.1109/PHM.2008.4711433

Rosenblatt, M. et al. (1956). Remarks on some nonparametric estimates of a density function. *Annals of Mathematical Statistics*, *27*(3), 832–837. doi:10.1214/aoms/1177728190

Saha, B., & Goebel, K. (2008). *Uncertainty management for diagnostics and prognostics of batteries using Bayesian techniques*. Paper presented at the Aerospace Conference. doi:10.1109/AERO.2008.4526631

Saltelli, A., Ratto, M., Andres, T., Campolongo, F., Cariboni, J., Gatelli, D., & Tarantola, S. (2008). *Global Sensitivity Analysis: The Primer*. Wiley-Interscience.

Sankararaman, S. (2014). (Already published). Significance, interpretation, and quantification of uncertainty in prognostics and remaining useful life prediction. *Mechanical Systems and Signal Processing*. (52)228-247

Sankararaman, S., Daigle, M., Saxena, A., & Goebel, K. (2013). *Analytical algorithms to quantify the uncertainty in remaining useful life prediction*. Paper presented at the Aerospace Conference. doi:10.1109/AERO.2013.6496971

Sankararaman, S., Daigle, M. J., & Goebel, K. (2014). Uncertainty Quantification in Remaining Useful Life Prediction Using First-Order Reliability Methods. *Reliability*. *IEEE Transactions on*, *63*(2), 603–619.

Sankararaman, S., Ling, Y., Shantz, C., & Mahadevan, S. (2009). *Uncertainty Quantification in Fatigue Damage Prognosis*. Paper presented at the Annual Conference of the PHM Society, PHM09, San Diego, CA.

Saxena, A., Celaya, J., Saha, B., Saha, S., & Goebel, K. (2010a). Metrics for Offline Evaluation of Prognostic Performance. *International Journal of the PHM Society*, *1*(1), 20.

Saxena, A., Celaya, J., Saha, B., Saha, S., & Goebel, K. (2010b). Metrics for Offline Evaluation of Prognostic Performance. *International Journal of Prognostics and Health Management*, *1*(1), 21.

Saxena, A., Celaya, J., Saha, S., Saha, B., Roychoudhury, I., & Goebel, K. (2010). *Requirements Specification for Prognostics Performance – An Overview*. Paper presented at the AIAA Infotech @ Aerospace, Atlanta, GA.

Saxena, A., Goebel, K., Larrosa, C. C., & Chang, F.-K. (2013). *CFRP Composites Dataset*. Retrieved from http://ti.arc.nasa.gov/project/prognostic-data-repository

Saxena, A., Roychoudhury, I., Celaya, J., Saha, B., Saha, S., & Goebel, K. (2012). *Requirement Flowdown for Prognostics Health Management.* Paper presented at the AIAA Infotech@Aerospace, Garden Grove, CA. doi:10.2514/6.2012-2554

Saxena, A., Shankararaman, S., & Goebel, K. (2014, July, 2014). *Performance Evaluation for Fleet-based and Unit-based Prognostic Methods.* Paper presented at the 2nd European Conference of the PHM Society, Nantes, France.

Talreja, R., & Singh, C. V. (2012). *Damage and failure of composite materials*. Cambridge University Press. doi:10.1017/CBO9781139016063

Tang, L., Kacprzynski, G. J., Goebel, K., & Vachtsevanos, G. (2009). *Methodologies for uncertainty management in prognostics*. Paper presented at the Aerospace conference.

Tanizaki, H., & Mariano, R. S. (1998). Nonlinear and non-Gaussian state-space modeling with Monte Carlo simulations. *Journal of Econometrics*, *83*(1), 263–290. doi:10.1016/S0304-4076(97)80226-6

Tvedt, L. (1989). *Second order reliability by an exact integral*. Springer. doi:10.1007/978-3-642-83828-6_26

Van Zandt, J. R. (2001). *A more robust unscented transform*. Paper presented at the International Symposium on Optical Science and Technology.

Wu, Y.-T. (1994). Computational methods for efficient structural reliability and reliability sensitivity analysis. *AIAA Journal*, *32*(8), 1717–1723. doi:10.2514/3.12164

KEY TERMS AND DEFINITIONS

Coverage: A quantitative measure expressed as the ratio of failures detected to the entire theoretically-detectable failure population.

Diagnosability: A measure for how well system faults can be detected and isolated without ambiguity given a system's definition and it sensors.

Diagnostics: Detection of anomaly or a fault and determining the possible locations and/or causes.

Failure Threshold: A design parameter specified to indicate maximum threshold beyond which a component is not expected to perform its intended function within specifications and/or is outside safe limits.

Fault Isolation: The process of determining the location of a fault to the extent necessary to effect repair.

Observability: A measure for how well internal states of a system can be inferred by knowledge of its external outputs measured through sensors.

Prognostics: Prediction of a system's future health states, degradation, and remaining useful life (RUL) based on its usage history and anticipated future load profile.